Caloric Restriction and Diet-Induced Weight Loss Do Not Induce Browning of Human Subcutaneous White Adipose Tissue in Women and Men with Obesity

Valentin Barquissau, Benjamin Léger, Diane Beuzelin, Frédéric F. Martins, Ez-Zoubir Amri, Didier Pisani, Wim H.M. Saris, Arne Astrup, Jean-José Maoret, Jason Iacovoni, et al.

Cell Reports

Resource

Caloric Restriction and Diet-Induced Weight Loss Do Not Induce Browning of Human Subcutaneous White Adipose Tissue in Women and Men with Obesity

Graphical Abstract

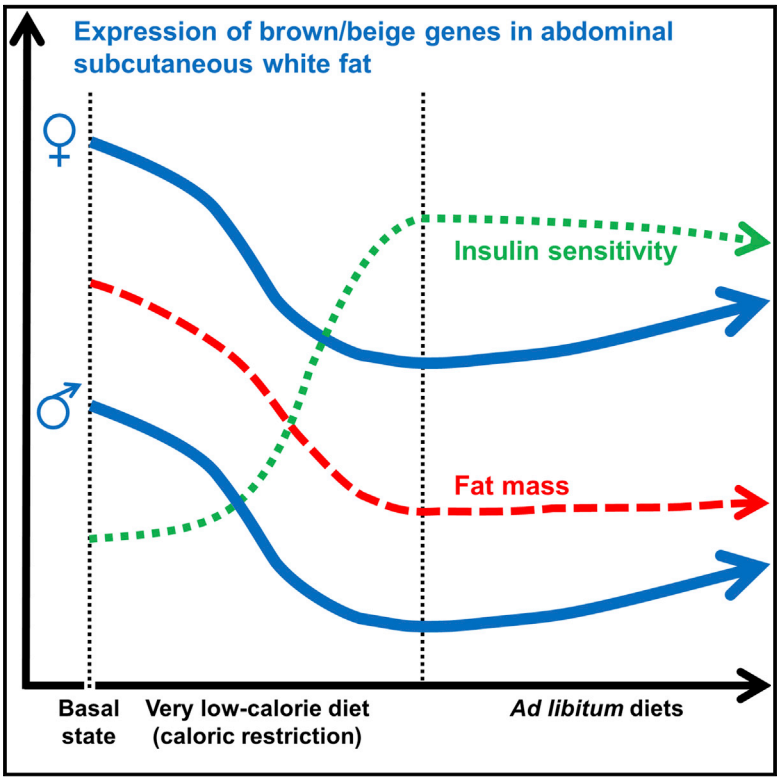

Authors

Valentin Barquissau, Benjamin Léger, Diane Beuzelin, ..., Cédric Moro, Nathalie Viguerie, Dominique Langin

Correspondence

dominique.langin@inserm.fr

In Brief

Barquissau et al. show that caloric restriction does not lead to browning of subcutaneous abdominal white adipose tissue in individuals with obesity. During a two-phase dietary intervention, changes in body fat and insulin resistance were independent of variations in subcutaneous abdominal white fat browning.

Highlights

- Subcutaneous abdominal fat is more brown-like in women than in men with obesity
- Caloric restriction diminishes browning features in subcutaneous abdominal fat
- Diet-induced changes in body fat are independent of subcutaneous abdominal WAT browning

Barquissau et al., 2018, Cell Reports *22*, 1079–1089
January 23, 2018
https://doi.org/10.1016/j.celrep.2017.12.102

CellPress

Cell Reports
Resource

Caloric Restriction and Diet-Induced Weight Loss Do Not Induce Browning of Human Subcutaneous White Adipose Tissue in Women and Men with Obesity

Valentin Barquissau,[1,2] Benjamin Léger,[1,2] Diane Beuzelin,[1,2] Frédéric Martins,[1,2] Ez-Zoubir Amri,[3] Didier F. Pisani,[3] Wim H.M. Saris,[4] Arne Astrup,[5] Jean-José Maoret,[1,2] Jason Iacovoni,[1,2] Sébastien Déjean,[2,6] Cédric Moro,[1,2] Nathalie Viguerie,[1,2] and Dominique Langin[1,2,7,8,*]

[1]INSERM, UMR 1048, Institute of Metabolic and Cardiovascular Diseases, Toulouse, France
[2]University of Toulouse, Paul Sabatier University, Toulouse, France
[3]University of Côte d'Azur, CNRS, Inserm, iBV, Nice, France
[4]Department of Human Biology, NUTRIM School of Nutrition and Translational Research in Metabolism, Maastricht University Medical Centre, Maastricht, the Netherlands
[5]Department of Nutrition, Exercise and Sports, Faculty of Sciences, University of Copenhagen, Copenhagen, Denmark
[6]CNRS, UMR 5219, Toulouse Mathematics Institute, Toulouse, France
[7]Toulouse University Hospitals, Laboratory of Clinical Biochemistry, Toulouse, France
[8]Lead Contact
*Correspondence: dominique.langin@inserm.fr
https://doi.org/10.1016/j.celrep.2017.12.102

SUMMARY

Caloric restriction (CR) is standard lifestyle therapy in obesity management. CR-induced weight loss improves the metabolic profile of individuals with obesity. In mice, occurrence of beige fat cells in white fat depots favors a metabolically healthy phenotype, and CR promotes browning of white adipose tissue (WAT). Here, human subcutaneous abdominal WAT samples were analyzed in 289 individuals with obesity following a two-phase dietary intervention consisting of an 8 week very low calorie diet and a 6-month weight-maintenance phase. Before the intervention, we show sex differences and seasonal variation, with higher expression of brown and beige markers in women with obesity and during winter, respectively. The very low calorie diet resulted in decreased browning of subcutaneous abdominal WAT. During the whole dietary intervention, evolution of body fat and insulin resistance was independent of changes in brown and beige fat markers. These data suggest that diet-induced effects on body fat and insulin resistance are independent of subcutaneous abdominal WAT browning in people with obesity.

INTRODUCTION

Dysregulated balance between energy intake and energy expenditure promotes storage of nutrient oversupply in white adipose tissue (WAT). An excess of fat mass is the hallmark of obesity, which leads to various metabolic disorders, such as cardiovascular diseases and type 2 diabetes. Achievement of negative energy balance through caloric restriction (CR) is a common strategy in the clinical management of obesity. CR-induced weight loss has been reported to reduce insulin resistance and improve most of the metabolic abnormalities seen in obesity (Andersen and Fernandez, 2013; Soare et al., 2014). It efficiently lowers diabetes risk (Hamman et al., 2006).

Targeting molecular pathways that regulate thermogenesis may provide a plausible means of increasing energy expenditure (Crowley et al., 2002; Giordano et al., 2016). Brown adipose tissue (BAT) has attracted much interest as the tissue controlling adaptive thermogenesis. Besides BAT depots at discrete anatomical sites, brown-like adipocytes, known as beige (or brite [brown-in-white]) adipocytes, have been identified within white fat depots, notably inguinal subcutaneous WAT in rodents. Mouse strains genetically prone to white fat browning are protected from obesity (Collins et al., 1997; Vitali et al., 2012), whereas high-fat-fed mice deficient for PRDM16, a transcriptional regulator driving browning, become obese and insulin resistant compared with wild-type mice (Cohen et al., 2014). In rodents, browning of WAT occurs in response to various stimuli, including cold (Cousin et al., 1992), pharmacological treatment (Himms-Hagen et al., 2000), and weight loss induced by surgery (Neinast et al., 2015). As the beneficial effects of CR have partly been ascribed to adaptations of energy-sensing pathways (Cantó and Auwerx, 2009), and as CR was recently reported to induce white fat browning in mice (Fabbiano et al., 2016), we hypothesized that browning of WAT in humans may be involved in the metabolic benefits elicited by CR. In this study, we therefore aimed to determine whether browning of WAT participates in changes in body fat induced by CR in people with obesity. First, we selected markers of brown, beige, and white adipocytes and established their cell specificity within human WAT. We then measured gene expression of the markers in the subcutaneous fat of 289 men and women with overweight and obesity from the DiOGenes (diet, obesity, and genes) trial at baseline, after an 8 week very low calorie diet (VLCD) and at the end of a 6 month follow-up period (Larsen et al., 2010). Expression of UCP1, the prototypical uncoupling protein responsible for dissipation of

Table 1. Top-Ranking Genes Displaying Highest Correlations with *UCP1* mRNA Level at Baseline (n = 289)

Gene Name	r	Bonferroni-Adjusted p Value
ELOVL3	0.56	$<10^{-22}$
CKMT2	0.55	$<10^{-21}$
CKMT1a	0.49	$<10^{-15}$
PPARGC1B	0.46	$<10^{-13}$
PCK1	0.40	$<10^{-9}$
PLIN5	0.32	$<10^{-5}$

the proton electrochemical gradient generated by the mitochondrial respiratory chain in brown adipocytes, and other brown fat markers showed higher expression in women than men and during winter compared with summer. During the negative energy balance phase induced by VLCD, a decrease in brown fat features was observed in subcutaneous fat. In the two phases of the dietary program, browning of WAT was not associated with loss of body fat and improvement of insulin sensitivity. Our data suggest that browning of subcutaneous abdominal fat does not participate in the beneficial effects of CR and diet-induced weight loss in humans.

RESULTS AND DISCUSSION

UCP1 mRNA Levels Are Correlated with Gene Expression of Thermogenic Markers but Not of Brown- and Beige-Specific Markers, in Human Subcutaneous Abdominal WAT

Numerous markers have been suggested to be specific to white, beige, and brown adipocytes. In addition to *UCP1*, we selected 90 genes related to the fat cell subtypes and adipose metabolism (Table S1). Because our major goal was to probe the extent of browning in a large biobank of human subcutaneous fat, we first determined whether these potential markers were preferentially expressed in adipocytes compared with other WAT cell types. To that end, subcutaneous abdominal fat samples from seven individuals were digested by collagenase to isolate mature adipocytes and stromavascular fraction cells. In order to focus on genes with robust fat cell expression, genes displaying more than 2-fold higher expression in the stromavascular fraction compared with mature adipocytes were removed in subsequent analyses. We also removed from the initial list genes whose expression levels were below the threshold of detection in more than 75% of DiOGenes trial fat samples. The final selection comprised 70 genes that were classified according to their expression in adipocyte subtypes as reported in the literature and according to our own published and unpublished datasets on human adipocytes converted *in vitro* in beige fat cells (Ahfeldt et al., 2012; Barquissau et al., 2016; Kazak et al., 2015; Lidell et al., 2013; Sharp et al., 2012; Waldén et al., 2012; Wu et al., 2012). The classification showed a large overlap between the categories, as only 3, 7, and 2 genes were classified as specific to white, beige, and brown adipocytes, respectively (Figure S1A; Table S1). Correlation matrix analysis of the 12 specific markers and *UCP1* in subcutaneous WAT from 289 DiOGenes trial participants at baseline showed weak association between *UCP1* and brown- and beige-specific markers in the context of whole human WAT (Figure S1B). Accordingly, the relevance of currently known brown- and beige-specific markers has been questioned, as they prove not to be robustly and consistently induced upon browning according to mouse strains, age of animals, and location of fat depots or when *in vivo* and *in vitro* browning of fat cells are compared (de Jong et al., 2015; Garcia et al., 2016). We therefore extended search for genes correlating with *UCP1* to the whole list (i.e., 70 genes) comprising several genes with well-known functions in brown fat metabolism. The highest correlations were found for *ELOVL3*, *CKMT2*, *CKMT1A, PPARGC1B*, *PCK1*, and *PLIN5* (Table 1). *ELOVL3* is a fatty acid elongase highly expressed in BAT (Tvrdik et al., 1997). Its expression is upregulated during browning of human adipocytes (Barquissau et al., 2016). CKMT-driven creatine cycle has recently been involved in a UCP1-independent thermogenic pathway (Bertholet et al., 2017; Kazak et al., 2015). *PPARGC1B* contributes to brown fat development (Uldry et al., 2006). *PLIN5* and *PCK1* are involved in metabolic pathways supporting thermogenic function (Barquissau et al., 2016; Wolins et al., 2006). Therefore, expression of *UCP1* and other genes with established functions in brown fat cells in this biobank of fat samples may not be incidental and may reflect the occurrence of bona fide thermogenic adipocytes in human subcutaneous abdominal WAT.

UCP1 Gene Expression in Subcutaneous Abdominal WAT Shows Large Inter-individual Variability and Is Sex and Season Dependent

At baseline, *UCP1* mRNA levels in subcutaneous WAT showed a wide range of expression, from the limit of detection to 500-fold higher. Hierarchical clustering of individuals according to *UCP1* mRNA levels distinguished three groups with high, medium, and low *UCP1* expression (Figures 1A and S1C). *ELOVL3*, *CKMT1a*, *CKMT2*, *PPARGC1B*, *PCK1*, and *PLIN5* displayed a gradually decreased expression in high, medium, and low *UCP1* groups (Figure 1A). Most of the correlations between these genes and *UCP1* were conserved when high/medium and low *UCP1* groups were analyzed separately (Table S2). *UCP1* mRNA level in females was 5-fold higher compared with males (Figure 1B). Higher gene expression in females than in males was also found for *ELOVL3*, *CKMT1a*, *CKMT2*, *PPARGC1B*, *PCK1*, and *PLIN5*. Most of the correlations between these genes and *UCP1* were significant in males and females (Table S2). Consistent with results in the entire set of patients (Figure 1A), differential expression of *UCP1* and associated markers in high-, medium-, and low-*UCP1* groups were preserved when males and females were separately analyzed (Figures S2A–S2G). Hence, there was a major distortion in sex distribution between groups: high- and medium-*UCP1* groups included 100% and 93% females, respectively, whereas the low-*UCP1* group was composed of 55% females and 45% males (Figure S2H). Such sex difference has been shown for active BAT, which is detected more frequently in females than in males (Cypess et al., 2009; Nookaew et al., 2013). As patients had been recruited all year round, we investigated the effect of seasons on expression of brown and beige fat markers. *UCP1* gene expression was

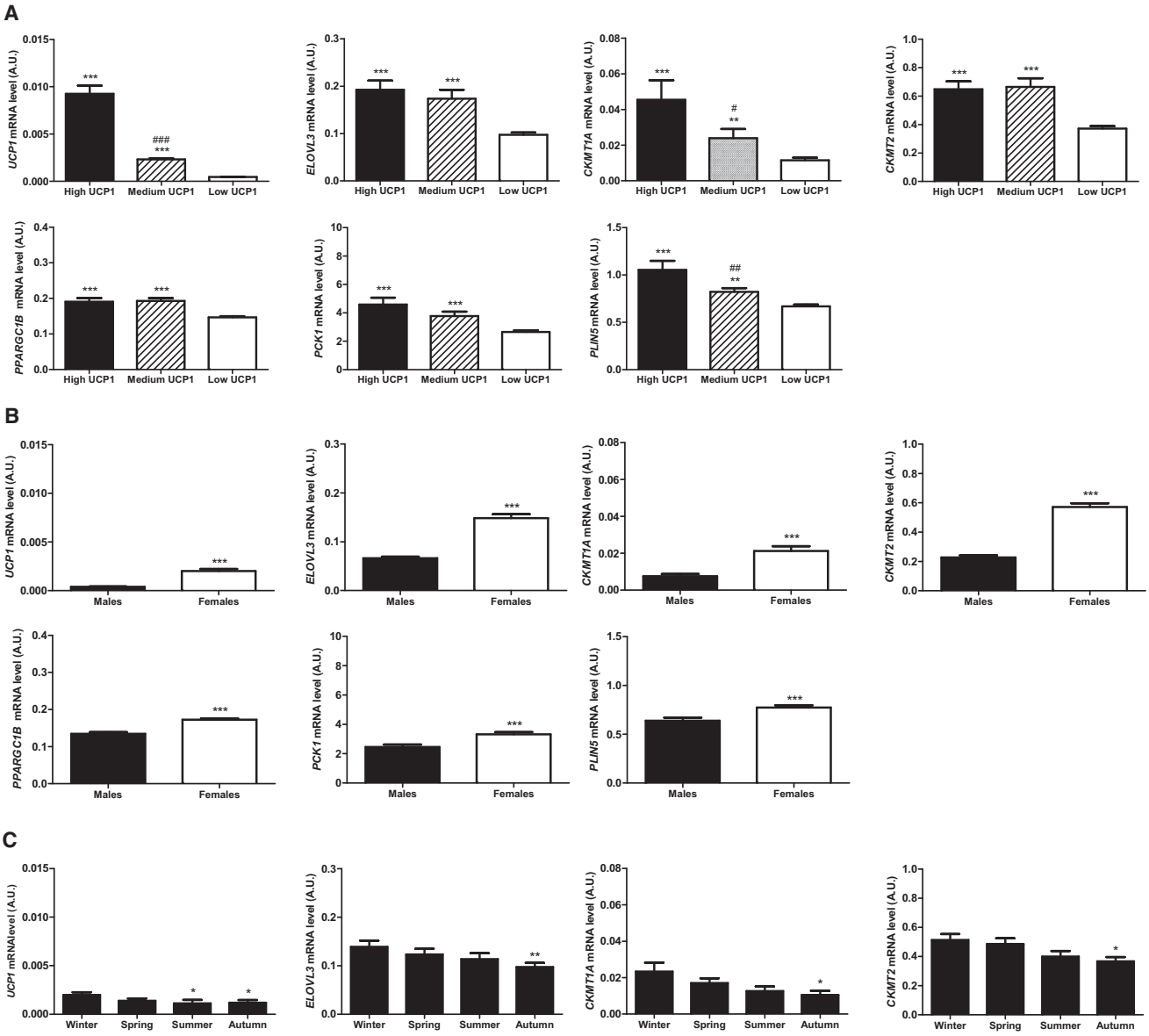

Figure 1. *UCP1* Gene Expression in Subcutaneous Abdominal White Adipose Tissue Shows Inter-individual Variability and Is Sex and Season Dependent

(A) *UCP1* and co-expressed gene mRNA levels in high (n = 20), medium (n = 59), and low (n = 210) *UCP1*-expressing groups at baseline.

(B) *UCP1* and co-expressed gene mRNA levels in males (n = 101) and females (n = 188).

(C) *UCP1* and co-expressed gene mRNA levels in individuals recruited in winter (n = 77), spring (n = 98), summer (n = 40), and autumn (n = 74).

Data are mean ± SEM. *p < 0.05, **p < 0.01, and ***p < 0.001 for high and medium versus low *UCP1* (A), for females versus males (B), and for summer and autumn versus winter (C); #p < 0.05, ##p < 0.01, and ###p < 0.001 for medium versus high UCP1 (A). See also Figures S1 and S2 and Table S2.

significantly lower in individuals recruited in summer and autumn compared with those recruited in winter (Figure 1C). A similar pattern was found for *ELOVL3*, *CKMT1a*, and *CKMT2*. These results suggest that browning of subcutaneous abdominal WAT, similarly to BAT activity, is higher in winter in humans (Au-Yong et al., 2009; Kern et al., 2014). Recruitment of males and females did not differ according to the recruitment season (Figure S2I), suggesting that sex differences were not biased by a seasonal effect.

Gene Expression of Brown and Beige Markers in Subcutaneous Abdominal WAT Is Decreased during CR

Next, we used the DiOGenes trial to investigate the relationship between CR and browning of WAT (Figure S3). The 8 week VLCD promoted substantial weight loss (−11%) and decrease in body fat and improved insulin sensitivity (Table 2; Figure 2A). Correlation matrix analysis of genes according to CR-induced changes revealed 11 clusters (Figure S4). One cluster included *UCP1*, *ELOVL3*, *CKMT1A*, and *CKMT2*. These genes showed

Table 2. Clinical Parameters of 289 Individuals with Obesity during the Two-Phase Dietary Intervention

	Baseline		End of VLCD		End of WMP	
	Males (n = 101)	Females (n = 188)	Males (n = 101)	Females (n = 188)	Males (n = 101)	Females (n = 188)
Age (years)	43.4 ± 5.9	41.7 ± 6.4	43.4 ± 5.9	41.7 ± 6.4	43.4 ± 5.9	41.7 ± 6.4
Weight (kg)	106.6 ± 17.3	95.0 ± 14.4	93.8 ± 15.3***	84.9 ± 13.0***	95.1 ± 16.2***	84.5 ± 13.3***
BMI (kg/m^2)	33.7 ± 4.6	34.5 ± 4.6	29.6 ± 4.1***	30.8 ± 4.2***	30.0 ± 4.2***	30.7 ± 4.4***
Body fat (%)	31.4 ± 6.8	43.5 ± 5.0	27.0 ± 5.7***	39.8 ± 5.6***	26.4 ± 5.6***	38.8 ± 6.1***
HOMA-IR	2.9 ± 1.7	2.3 ± 1.4	1.7 ± 1.1***	1.5 ± 0.9***	2.3 ± 2.3**	1.7 ± 1.1***

HOMA-IR, homeostatic model assessment of insulin resistance ([fasting glucose (mM) × fasting insulin (mU/L)/22.5]; VLCD, 8 week very low calorie diet; WMP, 6 month weight-maintenance phase. Data are mean ± SEM. **$p < 0.01$ and ***$p < 0.001$ for end of VLCD and end of WMP versus baseline. No significant difference was observed between end of VLCD and end of WMP.

decreased expression during VLCD (Figure 2B). Simultaneous downregulation of *UCP1* and *CKMTs* suggests that the two thermogenic pathways are diminished during CR. Another cluster composed of mitochondrial electron transport chain genes (namely, *NDUFA11*, *NDUFB6*, *CYC1*, *COX4I1*, and *COX8A*) showed the same pattern (Figure 2C). Downregulation of gene expression during CR was also found when males and females were analyzed separately (Figures S5A–S5C). Although season at recruitment influenced baseline expression of thermogenic markers, CR decreased expression of the genes independently of the season (Figure 3). These data reveal that CR decreases browning and the thermogenic potential of human subcutaneous abdominal WAT and show that CR-induced metabolic improvements in humans with obesity are not mediated by browning of this fat depot. This finding is coherent with the well-established decrease in resting metabolic rate and sympathetic nervous system activity observed during CR and weight loss in humans with obesity (Arone et al., 1995; Snitker et al., 2000; Clément et al., 2004; Heilbronn et al., 2006; Schwartz and Doucet, 2010). Accordingly, resting energy expenditure determined in 34 DiOGenes subjects by indirect calorimetry was significantly decreased ($p < 0.001$) during CR (data not shown). However, this observation of clinical relevance is opposite to what has recently been reported in mice (Fabbiano et al., 2016). The differences between mice and humans may partly be explained by an increased sensitivity to cold during fasting in mice that does not occur in humans in habitual living conditions (Cinti, 1999). Furthermore, the present study was focused exclusively on subcutaneous abdominal WAT. As human classical BAT depots were found to somewhat resemble murine beige inguinal WAT at a molecular level (Sharp et al., 2012; Shinoda et al., 2015; Wu et al., 2012), we cannot rule out that other fat pads (e.g., cervical, supraclavicular, or paravertebral depots) may display different responses to CR in humans.

Gene Expression of Brown and Beige Markers in Subcutaneous Abdominal WAT Does Not Follow Changes in Body Fat and Insulin Sensitivity during a Two-Phase Weight-Loss Dietary Program

We sought to investigate browning of WAT at baseline and at the end of the 8 month DiOGenes trial (Figure S3). Individuals were classified according to changes in *UCP1* gene expression between baseline and end of weight-maintenance phase (Figure 4A). Some individuals showed increases, whereas others showed no change or decreases in *UCP1* and browning marker expression (Figures 4A–4D, right, middle, and left, respectively). These inter-individual differences in WAT gene expression are coherent with the reported variability of response in BAT activity and WAT *UCP1* mRNA expression during weight loss of a few individuals (Oliveira et al., 2016; Orava et al., 2013; Rachid et al., 2015; Vijgen et al., 2012; Nakhuda et al., 2016). Despite markedly different regulation of gene expression, the decrease in body fat (12%–13%) was similar in the three groups (Figure 4E). Because the DiOGenes trial is composed of two phases, an initial 8 week VLCD phase and a 6 month weight-maintenance phase (Figure S3), we further explored the relationship between expression of the 70 selected genes and patterns of body fat during the two phases. The large number of individuals allowed cluster analysis of fat percentage trajectories (Figure S6A). Among the four profiles identified (Figure S6B), groups 1 and 2 showed similar adiposity at baseline but divergent responses (mild and pronounced body fat loss, respectively) to CR. During the follow-up period, groups 3 and 4 displayed opposite patterns, as group 3 regained body fat up to initial level, whereas group 4 further lost fat. The trajectory of the genes we identified as markers of browning (i.e., *UCP1*, *ELOVL3*, *CKMT1A*, and *CKMT2*) did not superimpose with the trajectory of body fat (Figures 5A–5D; Table S3). Two complementary multivariate analyses (partial least squares discriminant analysis [PLS-DA] and random forest) were applied in order to identify discriminating genes responsible for classification of patients into groups 1 or 2 during the VLCD phase and into groups 3 or 4 during the weight-maintenance phase (Breiman, 2001; Pérez-Enciso and Tenenhaus, 2003). *LEP* and *DPT* were identified within top-ranking genes by the two methods during CR and follow-up phases (Table S4). Fat percentage and *LEP* and *DPT* mRNA levels at baseline were similar in groups 1 and 2 (Figures 5E and 5F). After the VLCD, similar to variation in body fat, the decreases in *LEP* and *DPT* mRNA levels were more pronounced in group 2 than in group 1. During the follow-up period, the body fat return to baseline value in group 3 was associated with increased *LEP* expression. Conversely, body fat and *DPT* mRNA level simultaneously decreased in group 4 between the end of VLCD and the end of the protocol. The concordance in the evolution of body fat and leptin gene expression was expected and validated our methodology (Maffei et al., 1995). *DPT* encodes a non-collagenous component of the extracellular matrix, which is a white adipocyte-specific marker (Petrovic et al., 2010). As

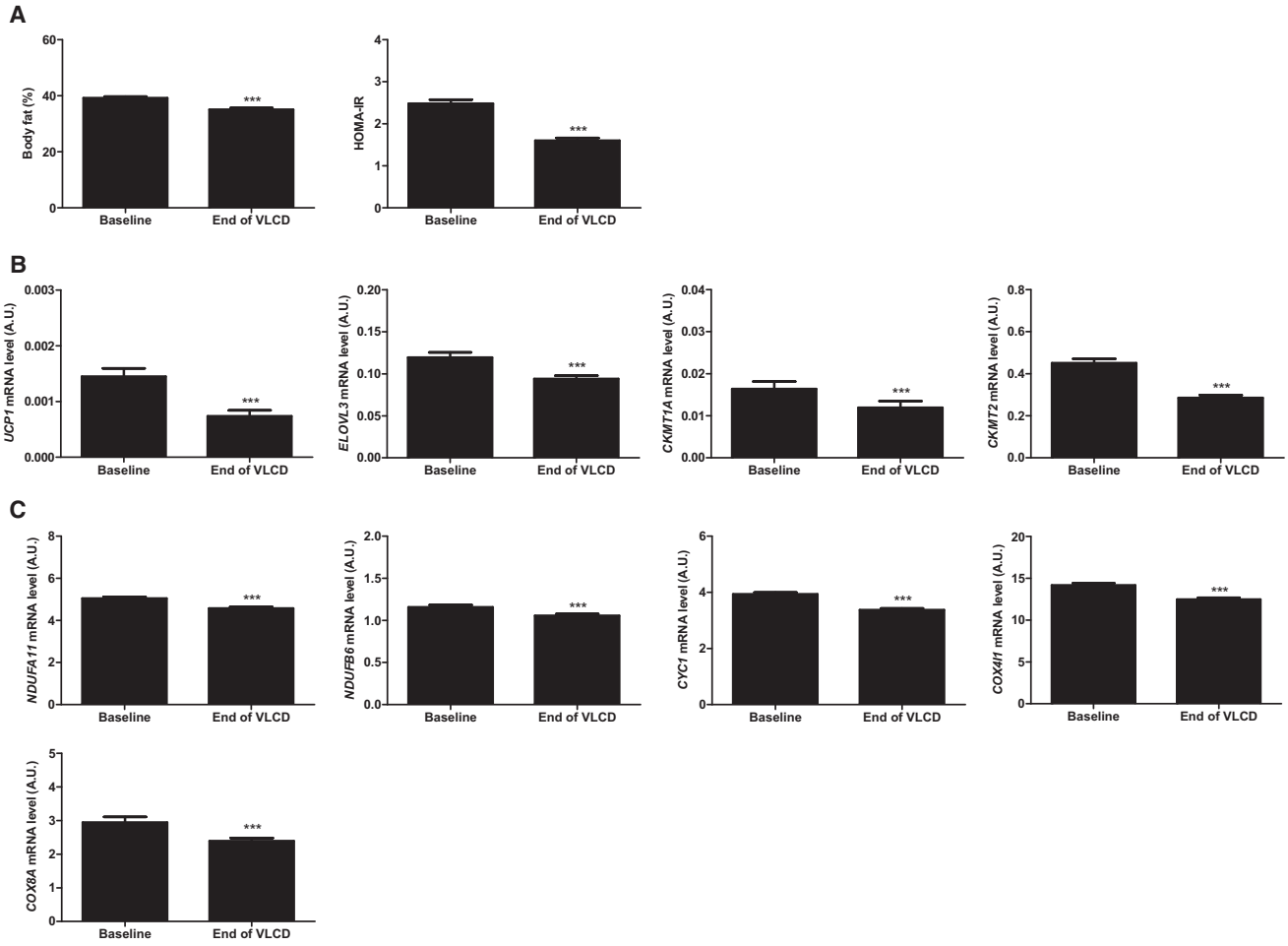

Figure 2. Expression of Browning Markers in Subcutaneous Abdominal White Adipose Tissue Is Decreased during Caloric Restriction

(A) Body fat and homeostatic model assessment of insulin resistance (HOMA-IR) before (baseline) and at the end of the 8 week very low calorie diet (VLCD).

(B) mRNA levels of *UCP1* and co-regulated brown fat markers.

(C) mRNA levels of mitochondrial electron transport chain subunits.

Data are mean ± SEM. ***p < 0.001 for end of VLCD versus baseline. See also Figures S3A, S4, and S5.

modifications in the composition of WAT extracellular matrix is a hallmark of obesity (Henegar et al., 2008), our data suggest that DPT might play a role in the remodeling of WAT during cycles of weight gain and loss.

A similar approach was used to identify genes whose expression was potentially associated with changes in the homeostatic model assessment of insulin resistance (HOMA-IR). Clustering of HOMA-IR trajectories identified three groups. Group 1 displayed high baseline values and a fall during VLCD, whereas groups 2 and 3 had lower baseline values with moderate decrease upon CR, leading to similar values in the three groups at the end of VLCD (Figures S6C and S6D). During weight maintenance, group 2 showed a further decrease in HOMA-IR, whereas groups 1 and 3 showed significant increases. Changes in expression of browning markers did not match changes in HOMA-IR (Figures S6E–S6H). Multivariate analyses did not identify genes robustly associated with changes in HOMA-IR (data not shown). These results suggest that subcutaneous abdominal WAT expression of the genes investigated in this study, including browning markers, is not associated with variation in insulin sensitivity during dietary intervention.

Relevance and Limitations of Studying Subcutaneous Abdominal WAT during a Large-Scale Dietary Intervention

Subcutaneous fat is by far the largest fat depot in the body and is worth investigating as such with respect to browning. Although visceral fat is also associated with impaired glucose metabolism, it is the subcutaneous abdominal fat region that supplies the major quantity of plasma free fatty acids implicated in metabolic abnormalities (Abate et al., 1995; Koutsari and Jensen, 2006). Of note, molecular adaptations in subcutaneous and visceral fat have the same discriminatory power with respect to insulin resistance, abdominal obesity, and metabolic syndrome despite a subset of genes being differentially expressed in the two depots (Klimcáková et al., 2011). Brown-like adipocytes in

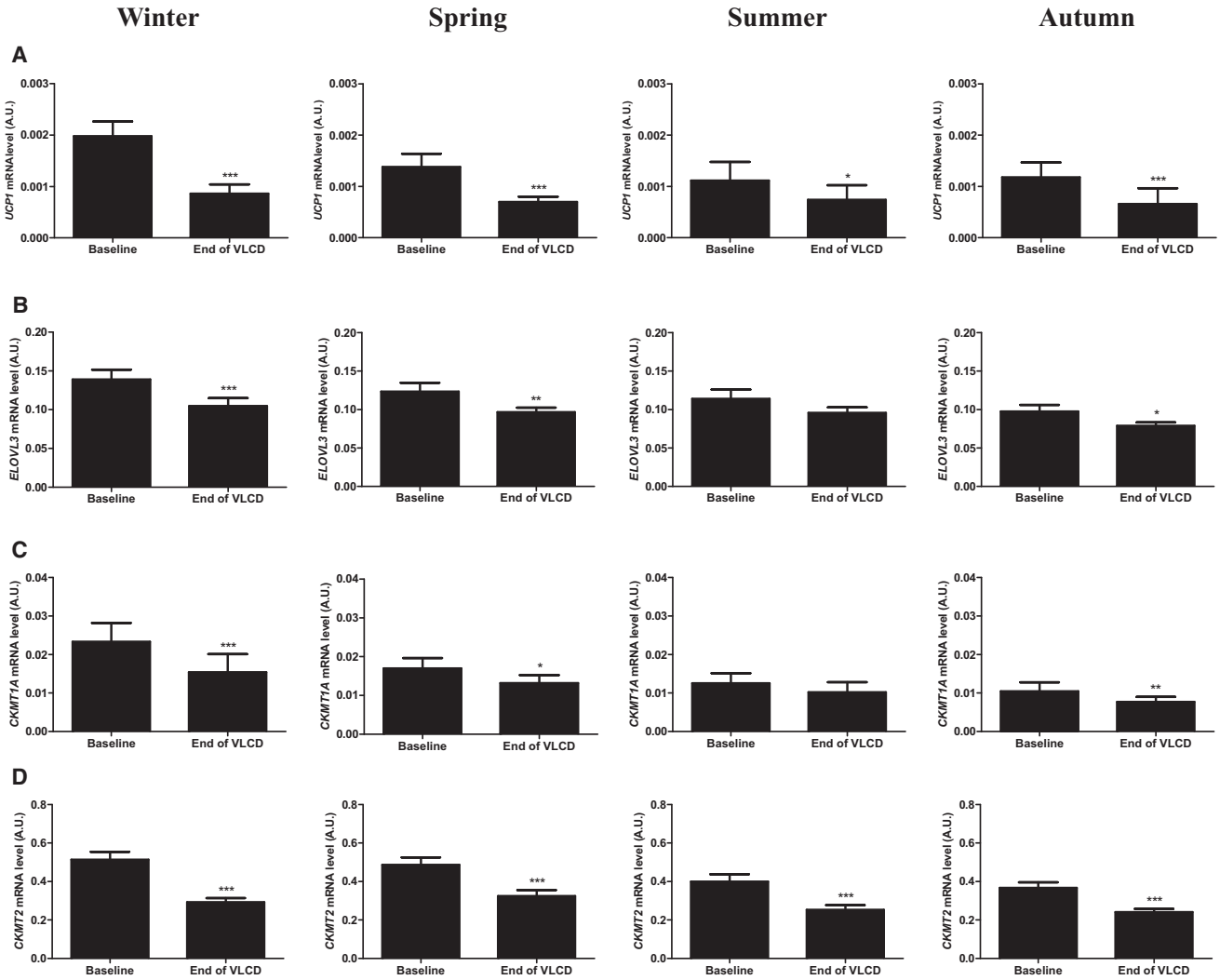

Figure 3. Caloric Restriction Regulates Expression of Browning Markers in Subcutaneous Abdominal White Adipose Tissue Independently of the Season

(A–D) mRNA levels of *UCP1* and co-regulated brown fat markers at baseline and at the end of the 8 week very low calorie diet (VLCD) in individuals recruited in winter (n = 77, left), spring (n = 98, middle left), summer (n = 40, middle right), and autumn (n = 74, right). (A) *UCP1*, (B) *ELOVL3*, (C) *CKMT1A*, and (D) *CKMT2* mRNA levels.

Data are mean ± SEM. *p < 0.05, **p < 0.01, and ***p < 0.001 for end of VLCD versus baseline. See also Figure S3A.

subcutaneous WAT favor oxidation of fatty acids and may limit their release into the circulation (Barquissau et al., 2016; Tiraby et al., 2003). We show here that this mechanism is unlikely to contribute to the beneficial effects of diet-induced weight loss. The present results may not be directly extrapolated to BAT depots such as supraclavicular fat (Cypess et al., 2013; Lidell et al., 2013; Jespersen et al., 2013). However, despite the marked heterogeneity in the occurrence of human brown and beige adipocytes according to anatomical location, similar regulation may be observed in BAT depots as those reported here in subcutaneous fat. Supporting this view, we show that subcutaneous abdominal WAT browning appears to be physiologically regulated by sex and season, similar to what has been observed in BAT (Au-Yong et al., 2009; Cypess et al., 2009; Kern et al., 2014; Nookaew et al., 2013). A limitation of the present study is its focus on a single WAT depot (i.e., the subcutaneous abdominal fat pad), which might be resistant to browning in humans contrary to rodents. However, it was recently reported that burn trauma patients showed browning of subcutaneous WAT after severe adrenergic stress (Sidossis et al., 2015). Pheochromocytoma and cancer-associated cachectic patients also displayed morphological and molecular features of beige fat in various abdominal fat depots (Frontini et al., 2013; Petruzzelli et al., 2014). Altogether, these results from independent groups suggest that human abdominal WAT depots are endowed with browning capacity and that stimuli (e.g., CR) are unlikely to induce "whitening" of subcutaneous abdominal WAT while promoting browning of other fat pads. As to whether the data

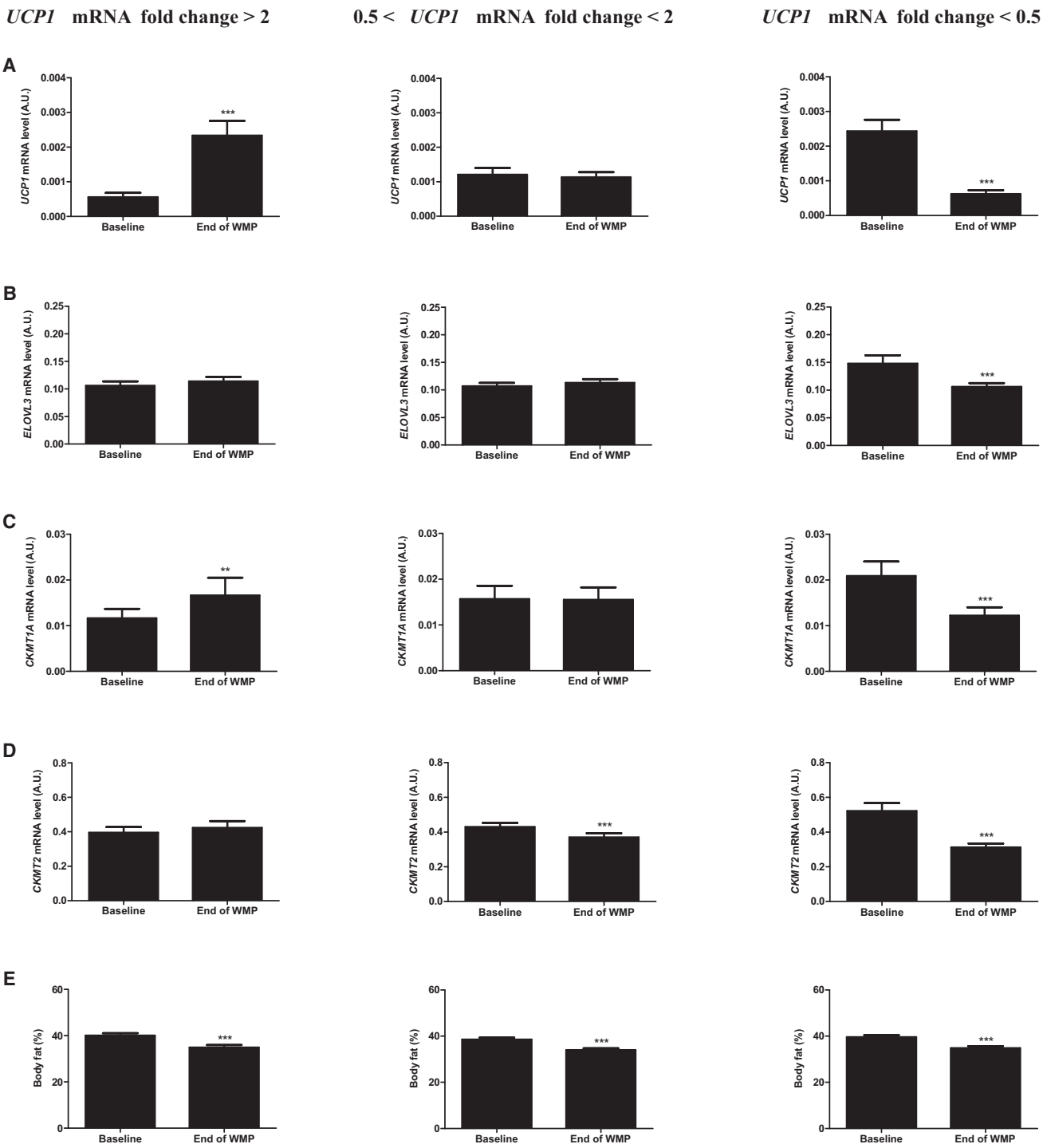

Figure 4. Changes in Expression of Browning Markers in Subcutaneous Abdominal White Adipose Tissue between Baseline and 6 Months after Caloric Restriction Display High Inter-individual Variability

(A–D) mRNA levels of *UCP1* and co-regulated brown fat markers at baseline and at the end of the weight-maintenance phase (WMP). (A) *UCP1*, (B) *ELOVL3*, (C) *CKMT1A*, and (D) *CKMT2* mRNA levels.

(E) Body fat percentage at baseline and at the end of WMP.

Data are mean ± SEM. **p < 0.01 and ***p < 0.001 for end of WMP versus baseline. See also Figure S3A.

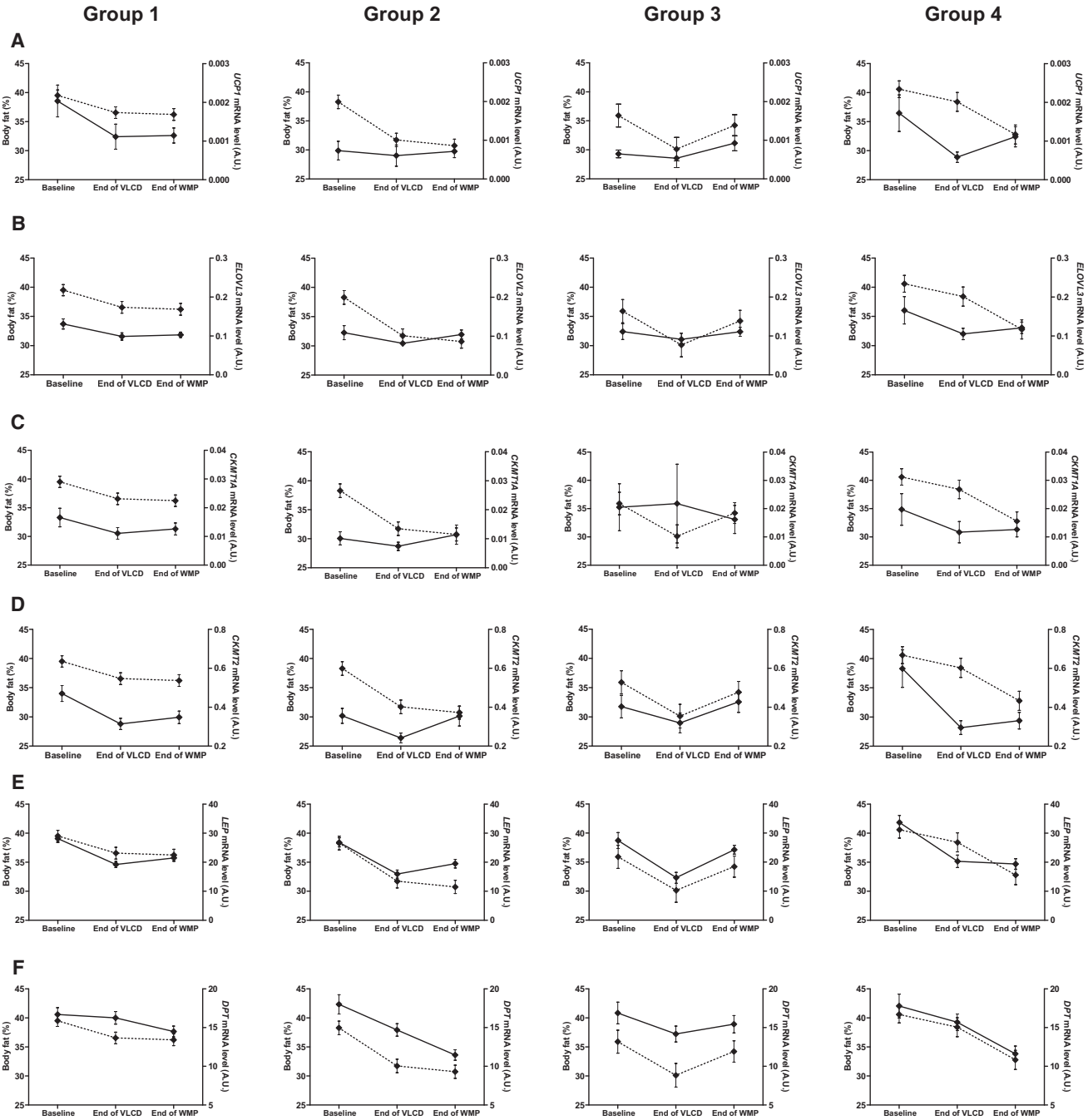

Figure 5. Expression of Browning Markers in Subcutaneous Abdominal White Adipose Tissue Does Not Follow Changes in Body Fat during a Two-Phase Weight Loss Dietary Program

(A–F) Variation in mRNA levels (full lines) according to four profiles of changes in fat percentage (dashed lines). (A) *UCP1*, (B) *ELOVL3*, (C) *CKMT1A*, (D) *CKMT2*, (E) *LEP*, and (F) *DPT* mRNA levels.

Data are mean ± SEM. Clustering of body fat percentage is shown in Figure S6. Statistical significance is provided in Table S4. VLCD, very low calorie diet; WMP, weight-maintenance phase. See also Figures S3A and S6 and Tables S3 and S4.

reported on diet-induced weight loss can be extrapolated to bariatric surgery-induced weight loss is a more challenging question. Indeed, several studies recently reported bariatric surgery-induced BAT activation and WAT browning in the neck region (Neinast et al., 2015; Oliveira et al., 2016; Rachid et al., 2015; Vijgen et al., 2012). Beyond the aforementioned hypothetical opposite response to CR of distinct WAT depots, these apparently contradictory findings may be accounted for by the

numerous physiological adaptations occurring after bariatric surgery in addition to the sole decrease in energy intake. Although CR per se is important, gastrointestinal hormones, bile acids, gut microbiota, and neurohormonal adaptations play specific roles in bariatric surgery-induced weight loss and improved glucose metabolism and may contribute to fat browning (Chondronikola et al., 2016; Liou et al., 2013; Neinast et al., 2015; Rachid et al., 2015; Vijgen et al., 2012). Future work investigating human fat samples from several anatomical locations during diet-induced energy deprivation, a technical and ethical challenge, would help establishing whether there is coordinated or differential response to CR of various fat depots with different thermogenic potentials.

In conclusion, studies on limited numbers of subjects may not be relevant given the large variability of fat browning in individuals with obesity. Investigating the relationship between browning markers and CR, body fat loss, and insulin sensitivity is possible only when several hundred individuals are investigated. Cellular markers previously identified as beige or brown specific have weak relevance *in vivo* in studying human whole WAT. Despite higher percentage of body fat, women with obesity display more browning features in subcutaneous abdominal WAT than men. CR is associated with impairment of browning in that fat depot. Whether this regulation is observed in other fat depots with higher content of brown and beige fat cells is not established. As CR simultaneously decreases adiposity and improves insulin sensitivity, the hypothesis of a contribution of subcutaneous abdominal WAT browning to weight loss-induced metabolic benefits proves not to be relevant in humans.

EXPERIMENTAL PROCEDURES

Further details and an outline of resources used in this work can be found in Supplemental Experimental Procedures.

DiOGenes Trial

DiOGenes was a multicenter dietary intervention study whose design has been previously described (Figure S3A) (Larsen et al., 2010). Briefly, adults with overweight and obesity participated in a dietary program with an 8 week VLCD (3.3–4.2 MJ/day). Volunteers with weight changes > 3 kg within 2 months prior to the beginning of CR were not included. Individuals achieving at least 8% of weight loss were randomized to a 6 month weight-maintenance phase with *ad libitum* diets. Five hundred forty-eight volunteers completed the whole intervention, and the present findings were obtained in 289 patients (Figure S3A), including 188 females (age 41.7 ± 6.4 years) and 101 males (age 43.4 ± 5.9 years). The study was approved by the local ethical committees in the respective countries in accordance with the Declaration of Helsinki. All study participants signed an informed consent document after verbal and written instructions that followed local legislation.

Quantification and Statistical Analysis

R software (version 3.2.2) was used for individuals' classification, random forests, and PLS-DA using different R packages (see below). Conventional statistical analyses were carried out using GraphPad Prism (version 5.0). Gaussian distribution of data were tested using the D'Agostino and Pearson omnibus test. Group comparisons were performed using one-way ANOVA (normally distributed data) or Kruskal-Wallis, Wilcoxon (paired data), and Mann-Whitney (unpaired data) tests (skewed data). Correlation coefficients were calculated using Pearson (normally distributed data) or Spearman (skewed data) correlations.

Hierarchical clustering analysis on *UCP1* mRNA levels was used to determine high, medium, and low *UCP1*-expressing groups. Euclidean distance was used as a measure of similarity, and Ward's method was chosen as agglomeration criteria. The dendrogram obtained was cut into three groups (Figure S1C). For body fat and HOMA-IR trajectories, grouping was performed among patients with available body fat or HOMA-IR data at each time points (n = 179 and 219, respectively) using hierarchical clustering analysis on a matrix composed of two synthetic variables, V1 and V2. V1 was calculated as the difference in body fat (or HOMA-IR) between end of VLCD and baseline and V2 as the difference in body fat (or HOMA-IR) between the end of the weight-maintenance phase and the end of VLCD. The dendrograms obtained for body fat and HOMA-IR were cut into four and three groups, respectively (Figures S6A and S6C). Groups were then hand-cleaned from borderline individuals and wrong group assignment on the basis of body fat (or HOMA-IR) trajectories to obtain more homogeneous clusters, resulting in a final analysis of 157 (181) individuals (Figures S6B and S6D).

Two multivariate discriminant analyses were used to identify the important variables (i.e., mRNA levels) for group classification: PLS-DA (R package mixOmics) and random forest (R package randomForest). PLS-DA is a PLS approach in which only one dependent variable represents the class or group membership (Pérez-Enciso and Tenenhaus, 2003). The variable influence on projection (VIP) indicates the influence of each variable on the discrimination between the different groups. Random forest is an ensemble of classification trees calculated on random subsets of the data, using a subset of randomly selected variables for each split in each classification tree (Breiman, 2001). Mean decreased Gini (MDG) is used as an indicator of importance of the variables. These two methods were chosen because of their complementarity: PLS-DA is a method taking place in a linear framework, whereas random forest is a nonlinear one. For each phase of the dietary intervention, the most important transcripts in the classification were ranked according to decreasing VIP or MDG. A classification score was calculated as the sum of the rank for each gene.

SUPPLEMENTAL INFORMATION

Supplemental Information includes Supplemental Experimental Procedures, six figures, and four tables and can be found with this article online at https://doi.org/10.1016/j.celrep.2017.12.102.

ACKNOWLEDGMENTS

We greatly thank Dr. Wouter van Marken Lichtenbelt (Maastricht University Medical Center) for helpful discussion. We are grateful to Marion Combes and Lucile Mir for expert technical assistance and to the GenoToul Genome and Transcriptome core facility. This work was supported by Inserm, Paul Sabatier University, Agence Nationale de la Recherche (ANR-12-BSV1-0025Obelip), Région Midi-Pyrénées (OBELIP and ILIP projects), the Commission of the European Communities (FP6-513946 DiOGenes and HEALTH-F2-2011-278373 DIABAT), and Innovative Medicines Initiative Joint Undertaking (grant agreement 31 115372). D.L. is a member of Institut Universitaire de France.

AUTHOR CONTRIBUTIONS

Conceptualization, V.B., N.V., and D.L.; Methodology, V.B., S.D., N.V., and D.L.; Investigation, V.B., D.B., F.M., W.H.M.S., A.A. and J.-J.M.; Formal Analysis, V.B., B.L., E.-Z.A., D.F.P., and J.I.; Writing – Original Draft, V.B. and D.L.; Writing – Review & Editing, V.B., B.L., D.B., F.M., E.-Z.A., D.F.P., W.H.M.S., A.A., J.-J.M., J.I., S.D., C.M., N.V., and D.L.; Funding Acquisition, W.H.M.S. and D.L.; Supervision, N.V. and D.L.

DECLARATION OF INTERESTS

The authors declare no competing interests.

Received: June 29, 2017
Revised: October 18, 2017
Accepted: December 27, 2017
Published: January 23, 2018

REFERENCES

Abate, N., Garg, A., Peshock, R.M., Stray-Gundersen, J., and Grundy, S.M. (1995). Relationships of generalized and regional adiposity to insulin sensitivity in men. J. Clin. Invest. *96*, 88–98.

Ahfeldt, T., Schinzel, R.T., Lee, Y.K., Hendrickson, D., Kaplan, A., Lum, D.H., Camahort, R., Xia, F., Shay, J., Rhee, E.P., et al. (2012). Programming human pluripotent stem cells into white and brown adipocytes. Nat. Cell Biol. *14*, 209–219.

Andersen, C.J., and Fernandez, M.L. (2013). Dietary strategies to reduce metabolic syndrome. Rev. Endocr. Metab. Disord. *14*, 241–254.

Arone, L.J., Mackintosh, R., Rosenbaum, M., Leibel, R.L., and Hirsch, J. (1995). Autonomic nervous system activity in weight gain and weight loss. Am. J. Physiol. *269*, R222–R225.

Au-Yong, I.T., Thorn, N., Ganatra, R., Perkins, A.C., and Symonds, M.E. (2009). Brown adipose tissue and seasonal variation in humans. Diabetes *58*, 2583–2587.

Barquissau, V., Beuzelin, D., Pisani, D.F., Beranger, G.E., Mairal, A., Montagner, A., Roussel, B., Tavernier, G., Marques, M.A., Moro, C., et al. (2016). White-to-brite conversion in human adipocytes promotes metabolic reprogramming towards fatty acid anabolic and catabolic pathways. Mol. Metab. *5*, 352–365.

Bertholet, A.M., Kazak, L., Chouchani, E.T., Bogaczynska, M.G., Paranjpe, I., Wainwright, G.L., Betourne, A., Kajimura, S., Spiegelman, B.M., and Kirichok, Y. (2017). Mitochondrial patch clamp of beige adipocytes reveals UCP1-positive and UCP1-negative cells both exhibiting futile creatine cycling. Cell Metab. *25*, 811–822.e4.

Breiman, L. (2001). Random forests. Mach. Learn. *45*, 5–32.

Cantó, C., and Auwerx, J. (2009). Caloric restriction, SIRT1 and longevity. Trends Endocrinol. Metab. *20*, 325–331.

Chondronikola, M., Harris, L.L., and Klein, S. (2016). Bariatric surgery and type 2 diabetes: are there weight loss-independent therapeutic effects of upper gastrointestinal bypass? J. Intern. Med. *280*, 476–486.

Cinti, S. (1999). The Adipose Organ (Kurtis).

Clément, K., Viguerie, N., Poitou, C., Carette, C., Pelloux, V., Curat, C.A., Sicard, A., Rome, S., Benis, A., Zucker, J.D., et al. (2004). Weight loss regulates inflammation-related genes in white adipose tissue of obese subjects. FASEB J. *18*, 1657–1669.

Cohen, P., Levy, J.D., Zhang, Y., Frontini, A., Kolodin, D.P., Svensson, K.J., Lo, J.C., Zeng, X., Ye, L., Khandekar, M.J., et al. (2014). Ablation of PRDM16 and beige adipose causes metabolic dysfunction and a subcutaneous to visceral fat switch. Cell *156*, 304–316.

Collins, S., Daniel, K.W., Petro, A.E., and Surwit, R.S. (1997). Strain-specific response to beta 3-adrenergic receptor agonist treatment of diet-induced obesity in mice. Endocrinology *138*, 405–413.

Cousin, B., Cinti, S., Morroni, M., Raimbault, S., Ricquier, D., Pénicaud, L., and Casteilla, L. (1992). Occurrence of brown adipocytes in rat white adipose tissue: molecular and morphological characterization. J. Cell Sci. *103*, 931–942.

Crowley, V.E., Yeo, G.S., and O'Rahilly, S. (2002). Obesity therapy: altering the energy intake-and-expenditure balance sheet. Nat. Rev. Drug Discov. *1*, 276–286.

Cypess, A.M., Lehman, S., Williams, G., Tal, I., Rodman, D., Goldfine, A.B., Kuo, F.C., Palmer, E.L., Tseng, Y.H., Doria, A., et al. (2009). Identification and importance of brown adipose tissue in adult humans. N. Engl. J. Med. *360*, 1509–1517.

Cypess, A.M., White, A.P., Vernochet, C., Schulz, T.J., Xue, R., Sass, C.A., Huang, T.L., Roberts-Toler, C., Weiner, L.S., Sze, C., et al. (2013). Anatomical localization, gene expression profiling and functional characterization of adult human neck brown fat. Nat. Med. *19*, 635–639.

de Jong, J.M., Larsson, O., Cannon, B., and Nedergaard, J. (2015). A stringent validation of mouse adipose tissue identity markers. Am. J. Physiol. Endocrinol. Metab. *308*, E1085–E1105.

Fabbiano, S., Suárez-Zamorano, N., Rigo, D., Veyrat-Durebex, C., Stevanovic Dokic, A., Colin, D.J., and Trajkovski, M. (2016). Caloric restriction leads to browning of white adipose tissue through type 2 immune signaling. Cell Metab. *24*, 434–446.

Frontini, A., Vitali, A., Perugini, J., Murano, I., Romiti, C., Ricquier, D., Guerrieri, M., and Cinti, S. (2013). White-to-brown transdifferentiation of omental adipocytes in patients affected by pheochromocytoma. Biochim. Biophys. Acta *1831*, 950–959.

Garcia, R.A., Roemmich, J.N., and Claycombe, K.J. (2016). Evaluation of markers of beige adipocytes in white adipose tissue of the mouse. Nutr. Metab. (Lond.) *13*, 24.

Giordano, A., Frontini, A., and Cinti, S. (2016). Convertible visceral fat as a therapeutic target to curb obesity. Nat. Rev. Drug Discov. *15*, 405–424.

Hamman, R.F., Wing, R.R., Edelstein, S.L., Lachin, J.M., Bray, G.A., Delahanty, L., Hoskin, M., Kriska, A.M., Mayer-Davis, E.J., Pi-Sunyer, X., et al. (2006). Effect of weight loss with lifestyle intervention on risk of diabetes. Diabetes Care *29*, 2102–2107.

Heilbronn, L.K., de Jonge, L., Frisard, M.I., DeLany, J.P., Larson-Meyer, D.E., Rood, J., Nguyen, T., Martin, C.K., Volaufova, J., Most, M.M., et al.; Pennington CALERIE Team (2006). Effect of 6-month calorie restriction on biomarkers of longevity, metabolic adaptation, and oxidative stress in overweight individuals: a randomized controlled trial. JAMA *295*, 1539–1548.

Henegar, C., Tordjman, J., Achard, V., Lacasa, D., Cremer, I., Guerre-Millo, M., Poitou, C., Basdevant, A., Stich, V., Viguerie, N., et al. (2008). Adipose tissue transcriptomic signature highlights the pathological relevance of extracellular matrix in human obesity. Genome Biol. *9*, R14.

Himms-Hagen, J., Melnyk, A., Zingaretti, M.C., Ceresi, E., Barbatelli, G., and Cinti, S. (2000). Multilocular fat cells in WAT of CL-316243-treated rats derive directly from white adipocytes. Am. J. Physiol. Cell Physiol. *279*, C670–C681.

Jespersen, N.Z., Larsen, T.J., Peijs, L., Daugaard, S., Homøe, P., Loft, A., de Jong, J., Mathur, N., Cannon, B., Nedergaard, J., et al. (2013). A classical brown adipose tissue mRNA signature partly overlaps with brite in the supraclavicular region of adult humans. Cell Metab. *17*, 798–805.

Kazak, L., Chouchani, E.T., Jedrychowski, M.P., Erickson, B.K., Shinoda, K., Cohen, P., Vetrivelan, R., Lu, G.Z., Laznik-Bogoslavski, D., Hasenfuss, S.C., et al. (2015). A creatine-driven substrate cycle enhances energy expenditure and thermogenesis in beige fat. Cell *163*, 643–655.

Kern, P.A., Finlin, B.S., Zhu, B., Rasouli, N., McGehee, R.E., Jr., Westgate, P.M., and Dupont-Versteegden, E.E. (2014). The effects of temperature and seasons on subcutaneous white adipose tissue in humans: evidence for thermogenic gene induction. J. Clin. Endocrinol. Metab. *99*, E2772–E2779.

Klimcáková, E., Roussel, B., Márquez-Quiñones, A., Kovácová, Z., Kováciková, M., Combes, M., Siklová-Vítková, M., Hejnová, J., Srámková, P., Bouloumié, A., et al. (2011). Worsening of obesity and metabolic status yields similar molecular adaptations in human subcutaneous and visceral adipose tissue: decreased metabolism and increased immune response. J. Clin. Endocrinol. Metab. *96*, E73–E82.

Koutsari, C., and Jensen, M.D. (2006). Thematic review series: patient-oriented research. Free fatty acid metabolism in human obesity. J. Lipid Res. *47*, 1643–1650.

Larsen, T.M., Dalskov, S.M., van Baak, M., Jebb, S.A., Papadaki, A., Pfeiffer, A.F., Martinez, J.A., Handjieva-Darlenska, T., Kunešová, M., Pihlsgård, M., et al.; Diet, Obesity, and Genes (Diogenes) Project (2010). Diets with high or low protein content and glycemic index for weight-loss maintenance. N. Engl. J. Med. *363*, 2102–2113.

Lidell, M.E., Betz, M.J., Dahlqvist Leinhard, O., Heglind, M., Elander, L., Slawik, M., Mussack, T., Nilsson, D., Romu, T., Nuutila, P., et al. (2013). Evidence for two types of brown adipose tissue in humans. Nat. Med. *19*, 631–634.

Liou, A.P., Paziuk, M., Luevano, J.M., Jr., Machineni, S., Turnbaugh, P.J., and Kaplan, L.M. (2013). Conserved shifts in the gut microbiota due to gastric bypass reduce host weight and adiposity. Sci. Transl. Med. *5*, 178ra41.

Maffei, M., Halaas, J., Ravussin, E., Pratley, R.E., Lee, G.H., Zhang, Y., Fei, H., Kim, S., Lallone, R., Ranganathan, S., et al. (1995). Leptin levels in human and

rodent: measurement of plasma leptin and ob RNA in obese and weight-reduced subjects. Nat. Med. *1*, 1155–1161.

Nakhuda, A., Josse, A.R., Gburcik, V., Crossland, H., Raymond, F., Metairon, S., Good, L., Atherton, P.J., Phillips, S.M., and Timmons, J.A. (2016). Biomarkers of browning of white adipose tissue and their regulation during exercise- and diet-induced weight loss. Am. J. Clin. Nutr. *104*, 557–565.

Neinast, M.D., Frank, A.P., Zechner, J.F., Li, Q., Vishvanath, L., Palmer, B.F., Aguirre, V., Gupta, R.K., and Clegg, D.J. (2015). Activation of natriuretic peptides and the sympathetic nervous system following Roux-en-Y gastric bypass is associated with gonadal adipose tissues browning. Mol. Metab. *4*, 427–436.

Nookaew, I., Svensson, P.A., Jacobson, P., Jernås, M., Taube, M., Larsson, I., Andersson-Assarsson, J.C., Sjöström, L., Froguel, P., Walley, A., et al. (2013). Adipose tissue resting energy expenditure and expression of genes involved in mitochondrial function are higher in women than in men. J. Clin. Endocrinol. Metab. *98*, E370–E378.

Oliveira, B.A., Pinhel, M.A., Nicoletti, C.F., Oliveira, C.C., Quinhoneiro, D.C., Noronha, N.Y., Marchini, J.S., Marchry, A.J., Junior, W.S., and Nonino, C.B. (2016). UCP1 and UCP3 expression is associated with lipid and carbohydrate oxidation and body composition. PLoS ONE *11*, e0150811.

Orava, J., Nuutila, P., Noponen, T., Parkkola, R., Viljanen, T., Enerbäck, S., Rissanen, A., Pietiläinen, K.H., and Virtanen, K.A. (2013). Blunted metabolic responses to cold and insulin stimulation in brown adipose tissue of obese humans. Obesity (Silver Spring) *21*, 2279–2287.

Pérez-Enciso, M., and Tenenhaus, M. (2003). Prediction of clinical outcome with microarray data: a partial least squares discriminant analysis (PLS-DA) approach. Hum. Genet. *112*, 581–592.

Petrovic, N., Walden, T.B., Shabalina, I.G., Timmons, J.A., Cannon, B., and Nedergaard, J. (2010). Chronic peroxisome proliferator-activated receptor gamma (PPARgamma) activation of epididymally derived white adipocyte cultures reveals a population of thermogenically competent, UCP1-containing adipocytes molecularly distinct from classic brown adipocytes. J. Biol. Chem. *285*, 7153–7164.

Petruzzelli, M., Schweiger, M., Schreiber, R., Campos-Olivas, R., Tsoli, M., Allen, J., Swarbrick, M., Rose-John, S., Rincon, M., Robertson, G., et al. (2014). A switch from white to brown fat increases energy expenditure in cancer-associated cachexia. Cell Metab. *20*, 433–447.

Rachid, B., van de Sande-Lee, S., Rodovalho, S., Folli, F., Beltramini, G.C., Morari, J., Amorim, B.J., Pedro, T., Ramalho, A.F., Bombassaro, B., et al. (2015). Distinct regulation of hypothalamic and brown/beige adipose tissue activities in human obesity. Int. J. Obes. *39*, 1515–1522.

Schwartz, A., and Doucet, E. (2010). Relative changes in resting energy expenditure during weight loss: a systematic review. Obes. Rev. *11*, 531–547.

Sharp, L.Z., Shinoda, K., Ohno, H., Scheel, D.W., Tomoda, E., Ruiz, L., Hu, H., Wang, L., Pavlova, Z., Gilsanz, V., and Kajimura, S. (2012). Human BAT possesses molecular signatures that resemble beige/brite cells. PLoS ONE *7*, e49452.

Shinoda, K., Luijten, I.H., Hasegawa, Y., Hong, H., Sonne, S.B., Kim, M., Xue, R., Chondronikola, M., Cypess, A.M., Tseng, Y.H., et al. (2015). Genetic and functional characterization of clonally derived adult human brown adipocytes. Nat. Med. *21*, 389–394.

Sidossis, L.S., Porter, C., Saraf, M.K., Børsheim, E., Radhakrishnan, R.S., Chao, T., Ali, A., Chondronikola, M., Mlcak, R., Finnerty, C.C., et al. (2015). Browning of subcutaneous white adipose tissue in humans after severe adrenergic stress. Cell Metab. *22*, 219–227.

Snitker, S., Macdonald, I., Ravussin, E., and Astrup, A. (2000). The sympathetic nervous system and obesity: role in aetiology and treatment. Obes. Rev. *1*, 5–15.

Soare, A., Weiss, E.P., and Pozzilli, P. (2014). Benefits of caloric restriction for cardiometabolic health, including type 2 diabetes mellitus risk. Diabetes Metab. Res. Rev. *30* (*Suppl 1*), 41–47.

Tiraby, C., Tavernier, G., Lefort, C., Larrouy, D., Bouillaud, F., Ricquier, D., and Langin, D. (2003). Acquirement of brown fat cell features by human white adipocytes. J. Biol. Chem. *278*, 33370–33376.

Tvrdik, P., Asadi, A., Kozak, L.P., Nedergaard, J., Cannon, B., and Jacobsson, A. (1997). Cig30, a mouse member of a novel membrane protein gene family, is involved in the recruitment of brown adipose tissue. J. Biol. Chem. *272*, 31738–31746.

Uldry, M., Yang, W., St-Pierre, J., Lin, J., Seale, P., and Spiegelman, B.M. (2006). Complementary action of the PGC-1 coactivators in mitochondrial biogenesis and brown fat differentiation. Cell Metab. *3*, 333–341.

Vijgen, G.H., Bouvy, N.D., Teule, G.J., Brans, B., Hoeks, J., Schrauwen, P., and van Marken Lichtenbelt, W.D. (2012). Increase in brown adipose tissue activity after weight loss in morbidly obese subjects. J. Clin. Endocrinol. Metab. *97*, E1229–E1233.

Vitali, A., Murano, I., Zingaretti, M.C., Frontini, A., Ricquier, D., and Cinti, S. (2012). The adipose organ of obesity-prone C57BL/6J mice is composed of mixed white and brown adipocytes. J. Lipid Res. *53*, 619–629.

Waldén, T.B., Hansen, I.R., Timmons, J.A., Cannon, B., and Nedergaard, J. (2012). Recruited vs. nonrecruited molecular signatures of brown, "brite," and white adipose tissues. Am. J. Physiol. Endocrinol. Metab. *302*, E19–E31.

Wolins, N.E., Quaynor, B.K., Skinner, J.R., Tzekov, A., Croce, M.A., Gropler, M.C., Varma, V., Yao-Borengasser, A., Rasouli, N., Kern, P.A., et al. (2006). OXPAT/PAT-1 is a PPAR-induced lipid droplet protein that promotes fatty acid utilization. Diabetes *55*, 3418–3428.

Wu, J., Boström, P., Sparks, L.M., Ye, L., Choi, J.H., Giang, A.H., Khandekar, M., Virtanen, K.A., Nuutila, P., Schaart, G., et al. (2012). Beige adipocytes are a distinct type of thermogenic fat cell in mouse and human. Cell *150*, 366–376.

Cell Reports, Volume *22*

Supplemental Information

Caloric Restriction and Diet-Induced Weight Loss Do Not Induce Browning of Human Subcutaneous White Adipose Tissue in Women and Men with Obesity

Valentin Barquissau, Benjamin Léger, Diane Beuzelin, Frédéric Martins, Ez-Zoubir Amri, Didier F. Pisani, Wim H.M. Saris, Arne Astrup, Jean-José Maoret, Jason Iacovoni, Sébastien Déjean, Cédric Moro, Nathalie Viguerie, and Dominique Langin

Supplemental figures

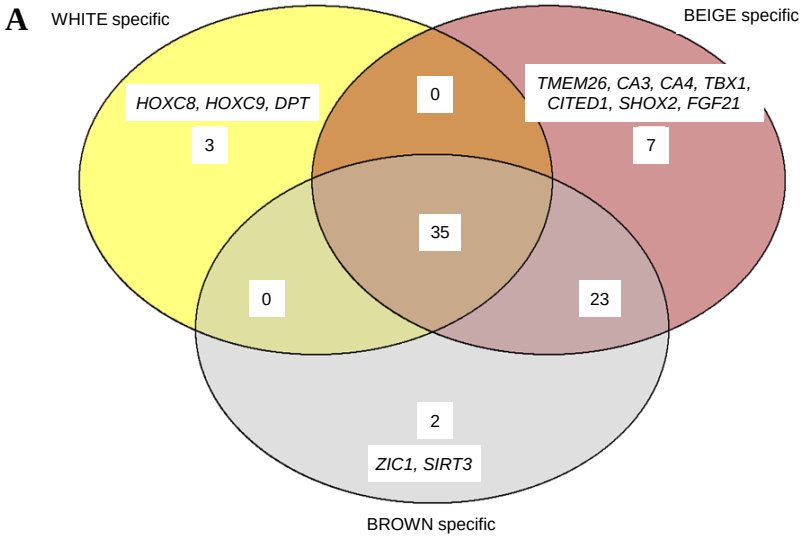

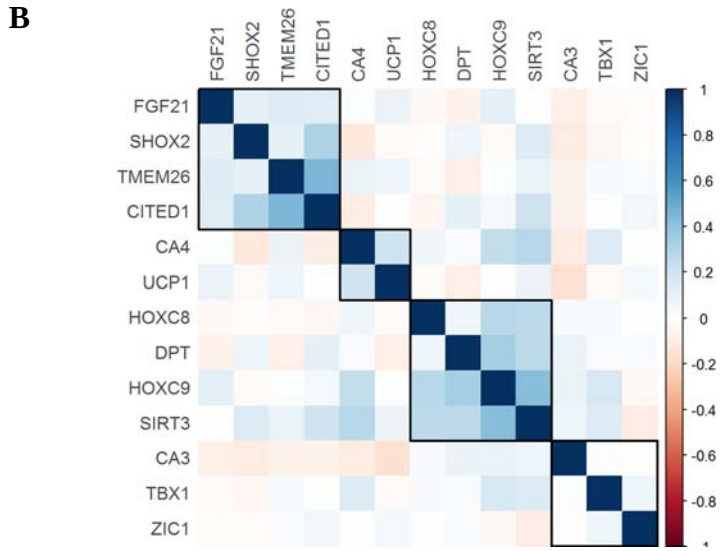

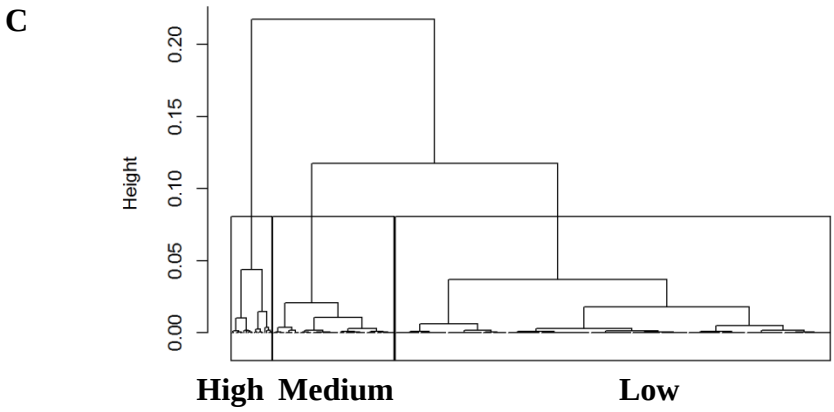

Supplemental Figure 1, related to Figure 1
(A) Venn diagram showing the number of genes specific of each adipocyte type according to the literature and this article data.
(B) Correlation matrix of the 12 cell type-specific markers and *UCP1*. Subsets of genes shown in boxes were identified by hierarchical clustering.
(C) Cluster dendrogram of *UCP1* gene expression in 289 individuals at baseline. Three groups with high, medium and low *UCP1* mRNA levels were defined.

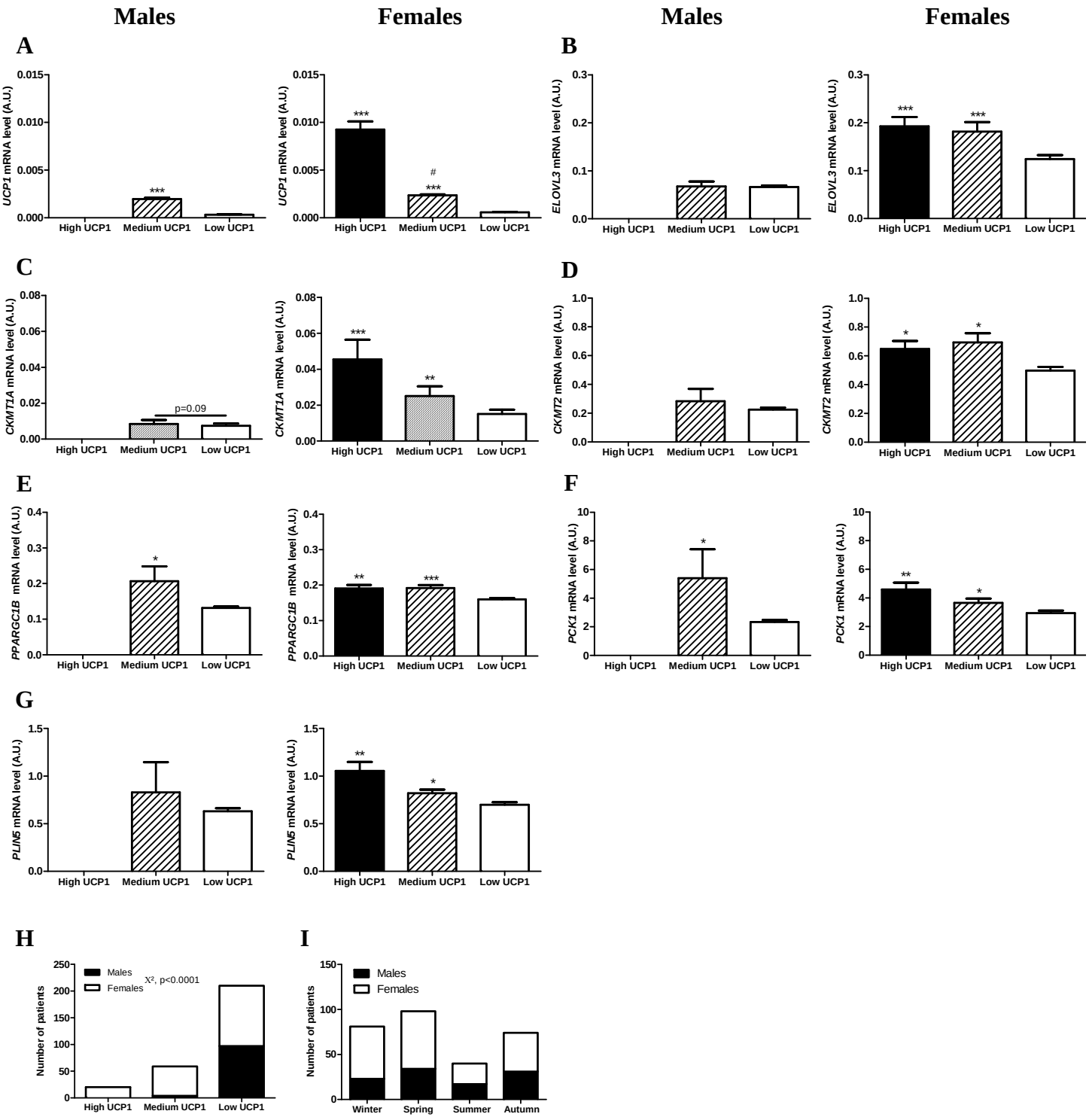

Supplemental Figure 2, related to Figure 1

(A-G) Sex effect on *UCP1* and co-expressed gene mRNA levels in high (n=0 and 20 in males and females, respectively), medium (n=4 and 55 in males and females, respectively) and low (n=97 and 113 in males and females, respectively) *UCP1* expressing groups. (A) *UCP1*, (B) *ELOVL3,* (C) *CKMT1A,* (D) CKMT2, (E) *PPARGC1B*, (F) *PCK1* and (G) *PLIN5* mRNA levels.
Data are means ± SEM. *, ** and ***: $p < 0.05$, 0.01 and 0.001 for high and medium *vs* low *UCP1;* #: $p < 0.05$ for medium *vs* high *UCP1*.

(H) Number of males and females in each *UCP1* group (white bars, females; black bars, males). Contingency analysis showed significant differential distribution of males and females. (I) Number of males and females recruited at different seasons (white bars, females; black bars, males). Contingency analysis showed no significantly different distribution of males and females.

A

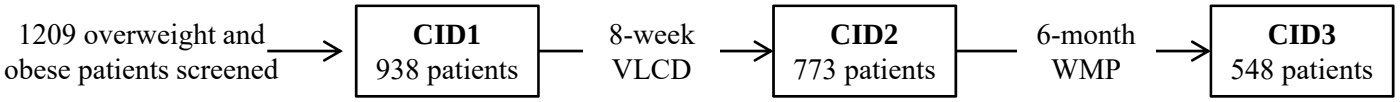

B

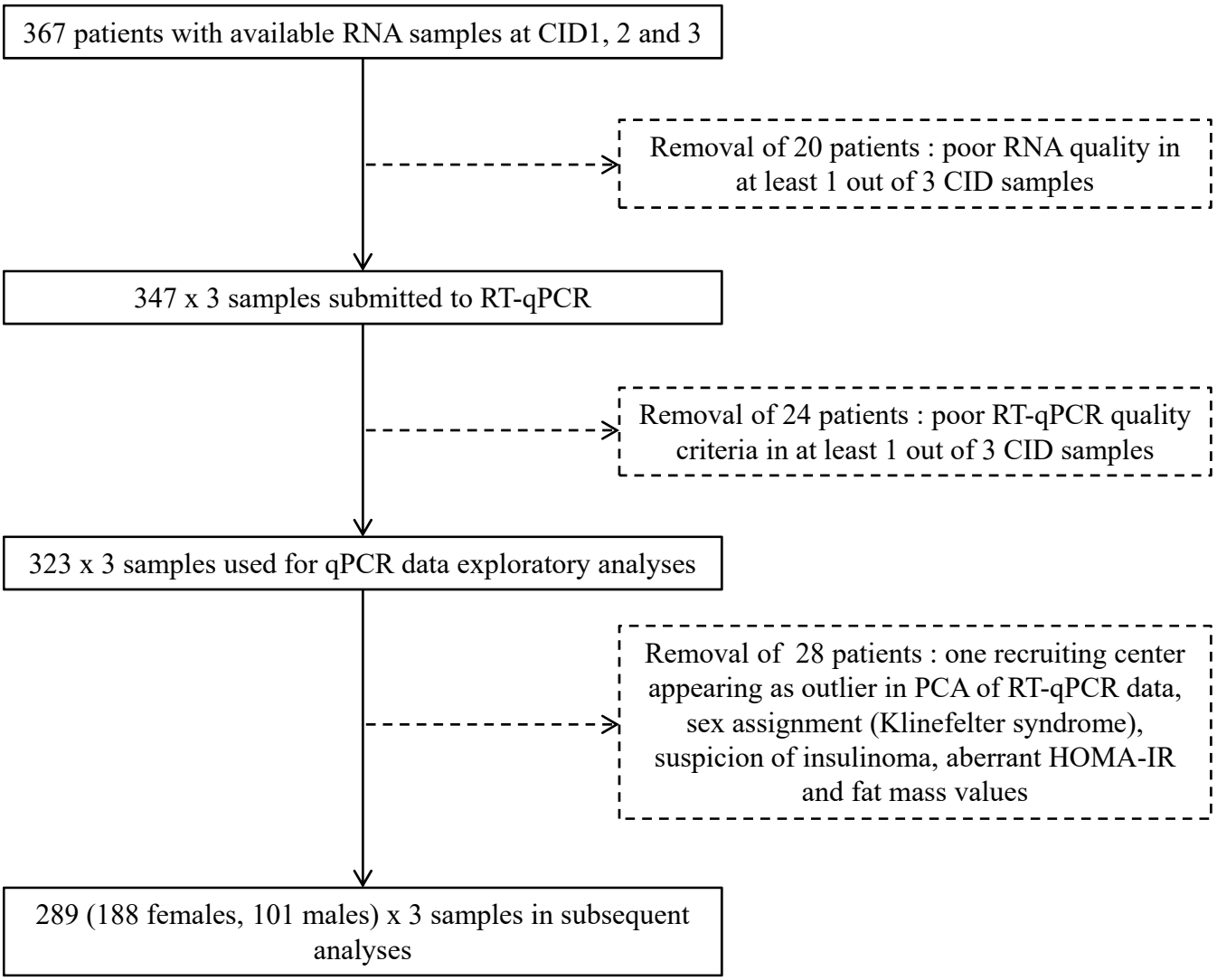

Supplemental Figure 3, related to Figures 2, 3, 4 and 5 and Table 2
(A) Overview of the DiOGenes protocol.
(B) Flowchart of patient and sample selection.
CID, clinical investigation day. PCA, principle component analysis. RT-qPCR, reverse transcription quantitative polymerase chain reaction. VLCD, very low calorie diet. WMP, weight maintenance phase.

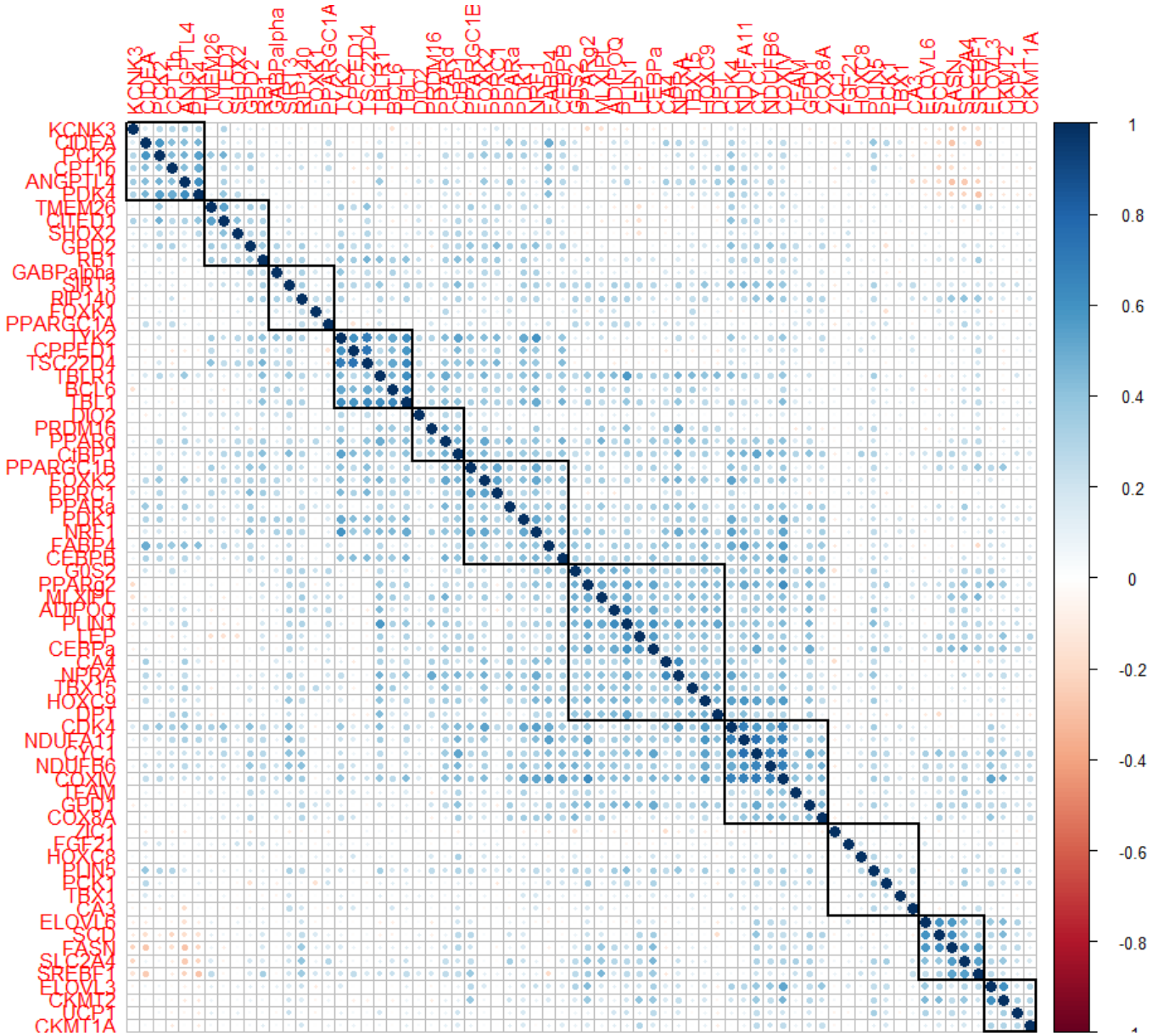

Supplemental Figure 4, related to Figure 2
Correlation matrix of changes in mRNA levels during very low calorie diet. Eleven clusters (boxes) were identified using a seriation algorithm to optimally reorder the genes and highlight the clusters.

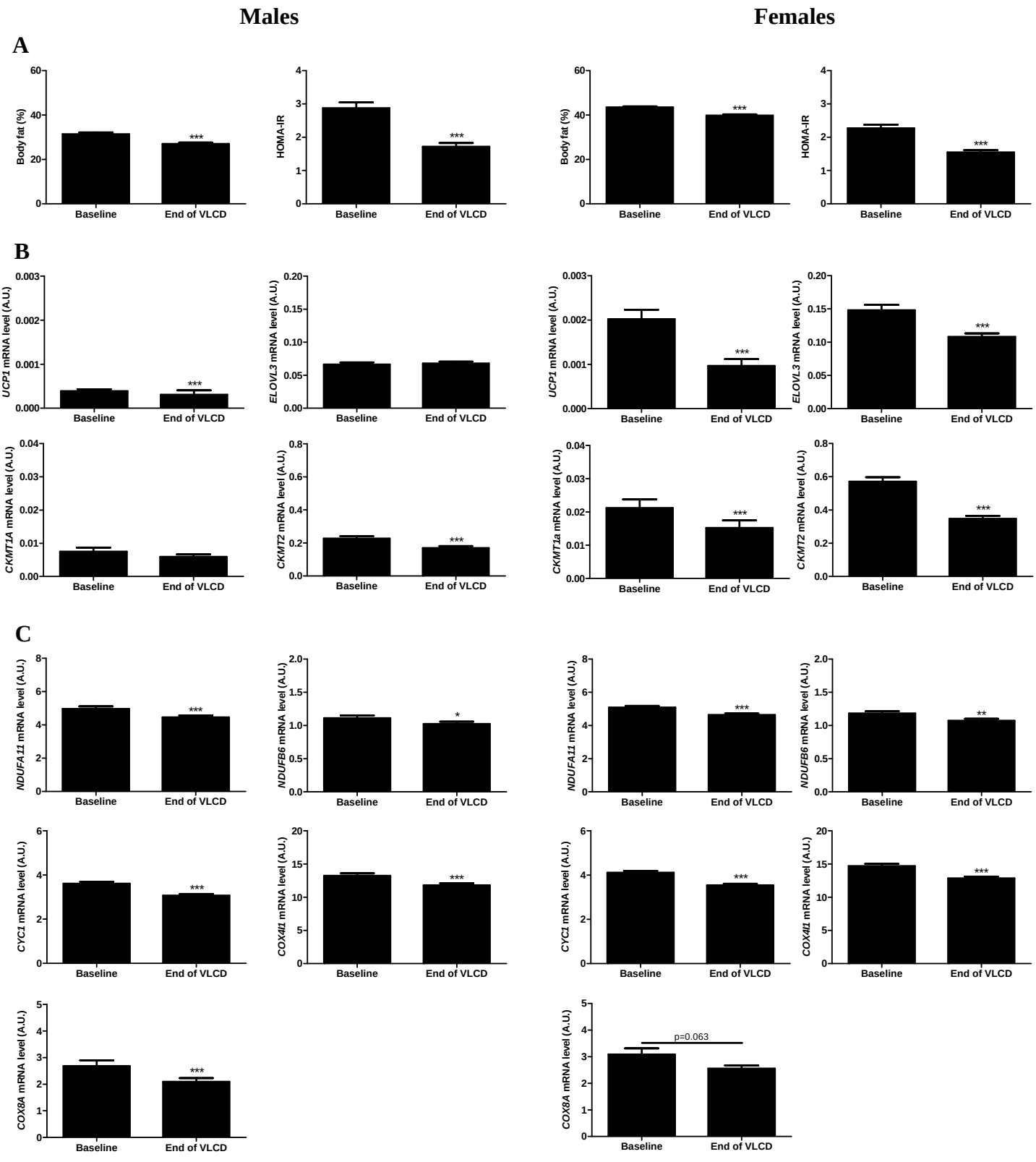

Supplemental Figure 5, related to Figure 2

(A) Body fat and homeostatic model assessment – insulin resistance (HOMA-IR) at baseline and at the end of 8-week very low calorie diet (VLCD) in males (left and middle-left panels and females (middle-right and right panels).

(B) mRNA levels of *UCP1* and co-regulated brown fat markers.

(C) mRNA levels of mitochondrial electron transport chain subunits.

Data are means ± SEM. *, ** and ***: $p < 0.05$, 0.01 and 0.001 for end of VLCD *vs* baseline.

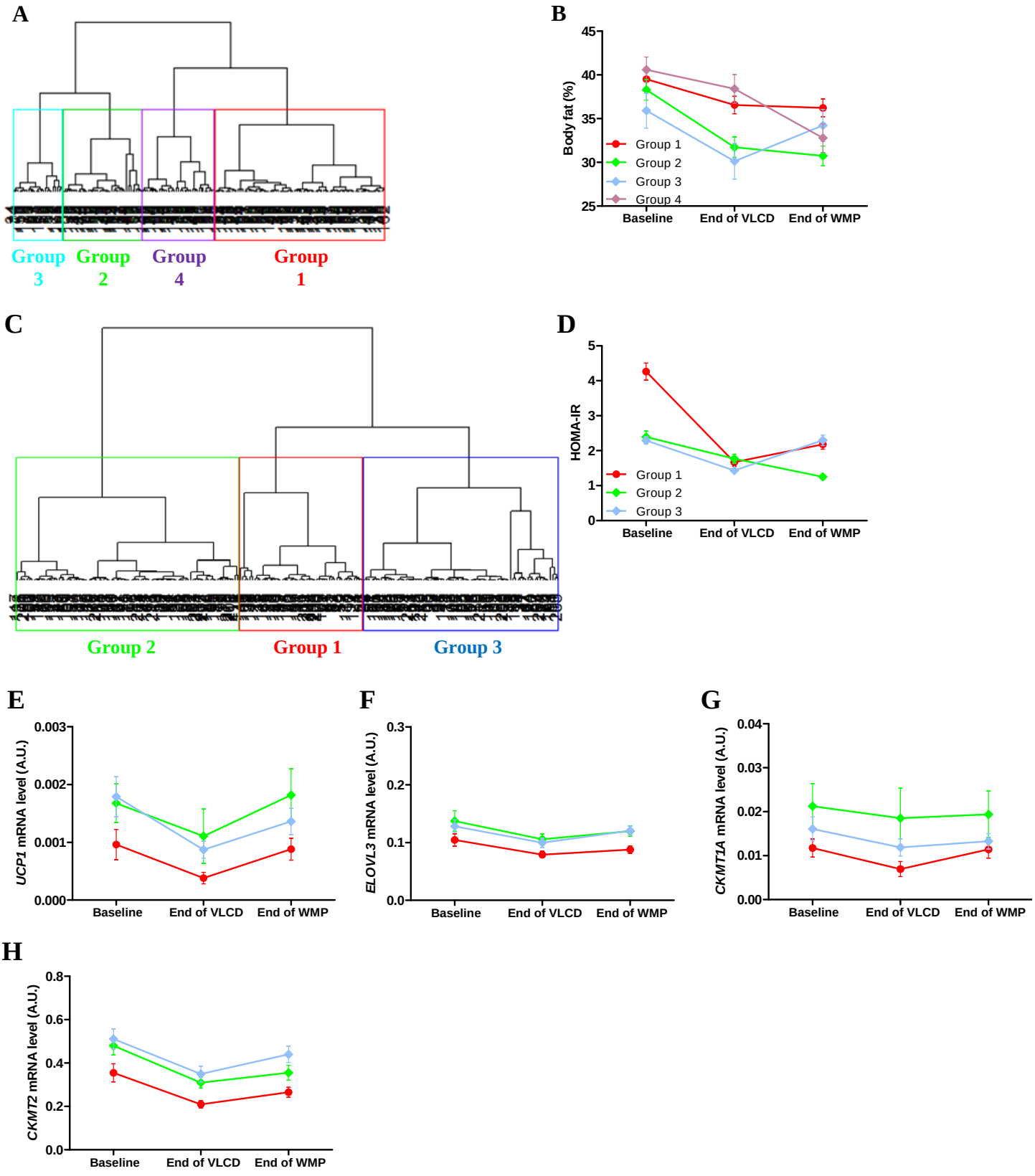

Supplemental Figure 6, related to Figure 5

(A,C) Cluster dendrograms of fat percentage (A) and HOMA-IR (C) trajectories between baseline and end of the two-phase dietary intervention.

(B) Profiles of changes in fat percentage in the four groups shown in A (n=72, 37, 24 and 24 in groups 1, 2, 3 and 4, respectively).

(D) Profiles of changes in HOMA-IR in the three groups shown in B (n=50, 53 and 78 in groups 1, 2 and 3, respectively).

(E-H) Variation in mRNA levels according to three profiles of changes in HOMA-IR identified in C-D. (E) *UCP1*, (F) *ELOVL3*, (G) *CKMT1A* and (H) *CKMT2* mRNA levels.

VLCD, very low calorie diet, WMP, weight maintenance phase. Data are means ± SEM.

Supplemental tables

Table S1. List of analysed genes, related to Method details and Figure S1A.

See content in accompanying Excel file.

Table S2. Correlation analyses between *UCP1* and co-expressed genes according to *UCP1* expression and sex at baseline, related to Figure 1.

	High and medium UCP1 expression (n=79)		Low UCP1 expression (n=210)		Males (n=101)		Females (n=188)	
Gene name	r	p value	r	p value	r	p value	r	p value
ELOVL3	0.35	$2*10^{-3}$	0.38	$< 10^{-8}$	0.10	0.34	0.47	$< 10^{-10}$
CKMT2	0.26	0.02	0.44	$< 10^{-10}$	0.21	0.04	0.37	$< 10^{-6}$
CKMT1A	0.29	0.01	0.34	$< 10^{-6}$	0.24	0.02	0.40	$< 10^{-7}$
PPARGC1B	0.17	0.13	0.31	$< 10^{-5}$	0.32	10^{-3}	0.34	$< 10^{-5}$
PCK1	0.32	$4*10^{-3}$	0.27	$< 10^{-4}$	0.27	$6*10^{-3}$	0.35	$< 10^{-6}$
PLIN5	0.31	$6*10^{-3}$	0.15	0.03	0.14	0.16	0.32	$< 10^{-5}$

Table S3. Statistical analyses, related to Figure 5.

	Cluster 1 (n=72)			Cluster 2 (n=37)		Cluster	3 (n=24)		Cluster	4 (n=24)		
	Baseline *vs* end of VLCD	Baseline *vs* end of WMP	End of VLCD *vs* end of WMP	Baseline *vs* end of VLCD	Baseline *vs* end of WMP	End of VLCD vs end of WMP	Baseline *vs* end of VLCD	Baseline *vs* end of WMP	End of VLCD *vs* end of WMP	Baseline *vs* end of VLCD	Baseline *vs* end of WMP	End of VLCD *vs* end of WMP
Body fat (%)	< 0.001	< 0.001	ns	< 0.001	< 0.001	ns	<0.001	<0.05	< 0.001	< 0.05	< 0.001	< 0.001
UCP1	< 0.001	< 0.01	< 0.05	ns	ns	ns	ns	ns	< 0.05	ns	ns	ns
ELOVL3	< 0.05	ns	ns ns ns ns ns ns ns <							0.05	ns	ns
CKMT1a	< 0.05	ns	ns ns ns ns ns ns ns ns ns ns									
CKMT2	< 0.001	< 0.001	ns	< 0.001	ns	< 0.01	ns	ns	< 0.001	< 0.001	< 0.001	ns
LEP	< 0.001	< 0.001	Ns	< 0.001	< 0.001	ns	< 0.001	ns	< 0.001	< 0.001	< 0.001	ns
DPT	ns	< 0.001	<0.001	ns	< 0.001	< 0.001	ns	ns	ns	ns	< 0.001	< 0.01

VLCD, very low calorie diet. WMP, weight maintenance phase. ns, non significant (p value > 0.05)

Table S4. Multivariate analyses according to the four profiles defined by cluster analysis of body fat evolution during the multiple phase dietary intervention, related to Figure 5.

	Gene name	PLS-DA rank	RF rank	Combined rank
Discrimination between groups 1 and 2 who showed similar body fat at baseline but divergent body fat loss, during very low calorie diet	*RIP140*	4	2	1
	DPT	1	6	2
	LEP	5	4	3
	CKMT2	6	5	4
	ELOVL3	2	10	5
Discrimination between group 3 who regained body fat and group 4 who lost body fat during ad libitum follow up diets	*LEP*	1	1	1
	DPT	2	2	2
	CA3	3	3	3
	ANGPTL4	4	4	4
	NDUFB6	5	6	5

PLS-DA, partial least quare discriminant analysis. RF, random forest

Supplemental experimental procedures

Further information and requests for resources and reagents should be directed to and will be fulfilled by the Lead Contact, Dominique Langin (dominique.langin@inserm.fr).”

Experimental models and subject details

Additional human fat samples for cell type isolation

Abdominal subcutaneous adipose tissue samples were obtained from 6 women and 1 men (age 40 ± 1.1 years, BMI 25 ± 0.8 kg/m²) undergoing abdominal dermolipectomy at Rangueil university hospital, Toulouse, France. None of the patients had recent large variations in body weight. The volunteers signed informed consent for an anonymous use of samples.

hMADS adipocyte culture and browning

Human multipotent adipose-derived stem (hMADS) cells established from the prepubic fat pad of a 4-month-old male were cultured and differentiated into white adipocytes within 14 days. Browning of white adipocytes was induced by addition of rosiglitazone between day 14 and day 18 (Barquissau et al., 2016). Six independent replicates of both white and beige fat cells were harvested for RNA extraction at day 18.

Method details

DiOGenes investigation days

At each clinical investigation day (i.e., at baseline, after VLCD and after weight maintenance phase), bio-clinical data were collected, blood was sampled and a needle biopsy of abdominal subcutaneous WAT was performed in the morning after overnight fast. Body fat was assessed with the use of dual-energy x-ray absorptiometry or bioelectrical impedance analysis.

Adipocyte and stromavascular cell isolation

Adipose tissue was cleaned and digested by collagenase as previously described (Klimcakova et al., 2011).

RNA extraction

Fat samples from DiOGenes trial were processed following an in-house optimized protocol for total RNA preparation (Viguerie et al., 2012). Briefly, frozen AT sample was homogenized in QIAzol (Qiagen) using a rotor-stator homogenizer until homogeneity. After addition of chloroform and centrifugation, the aqueous phase was transferred onto column (RNeasy mini kit, Qiagen) and processed following manufacturer instructions.

Separated mature adipocytes, stromavascular cells and hMADS adipocytes were collected for total RNA extraction using RNeasy mini kit (Qiagen).

Gene expression analysis from human adipose tissue and cell samples

RNA quality of human and cell samples was checked by capillary electrophoresis (Experion, Bio-Rad). cDNA synthesis (High-Capacity cDNA Reverse Transcription Kit, Applied Biosystems) and massive parallel real-time PCR using the Biomark HD system with 96.96 Dynamic Array IFC (Fluidigm) and TaqMan assays (Applied Biosystems) were performed as described (Viguerie et al., 2012). Using geNorm software, *PUM1* was identified as the most stable gene among the whole gene set (including 3 potential housekeeping genes: *PUM1*, *LRP10* and *GUSB*) and used as reference gene to normalize mRNA levels using the $2^{-\Delta Ct}$ method.

Gene selection and classification

Ninety genes related to adipose metabolism and to adipocyte subtype identity were selected (Table S1). Genes reported in the literature to discriminate between white, beige and brown adipocytes were included in the "white-", "beige-" and "brown-fat marker" categories, respectively. Classical and recently described thermogenic and oxidative markers, as well as genes up-regulated during browning of hMADS cells were grouped in the "brown-beige fat marker" category. Additional genes that could play a role in adipose metabolism, which were not significantly increased in hMADS cells after browning and which were not found in the literature to be specifically enriched in one adipose subtype, were considered as "adipocyte markers". Genes supposed to belong to one of the above categories but showing higher expression in stromavascular fraction cells (stromavascular fraction *vs* adipocyte ratio > 2) were classified in the "stromavascular fraction cell marker" category.

Resource table

REAGENT or RESOURCE	SOURCE	IDENTIFIER
Biological Samples		
DiOGenes adipose tissue RNA samples	Prof. Dominique Langin on behalf of the DiOGenes consortium	Dominique.Langin@inserm.fr
Chemicals, Peptides, and Recombinant Proteins		
QIAzol	Qiagen	Cat#79306
Critical Commercial Assays		
RNeasy mini kit	Qiagen	Cat#74106
High-Capacity cDNA Reverse Transcription Kit	Thermo Fischer Scientific	Cat#4368814
PreAmp Master Mix kit	Fluidigm	PN 100-5581
TaqMan Universal PCR Master Mix kit	Thermo Fischer Scientific	PN 4304437
Experimental Models: Cell Lines		
Human Multipotent Adipose-Derived Stem cells	Dr. Ez-Zoubir Amri, Nice, France	Ez-Zoubir.AMRI@unice.fr
Oligonucleotides		
Taqman assays for qPCR	Thermo Fischer Scientific	See Table S1
Software and Algorithms		
geNorm software	(Vandesompele et al., 2002)	https://genorm.cmgg.be/
GraphPad Prism software, version 5.0	GraphPad Software	https://www.graphpad.com/scientific-software/prism/
R software, version 3.2.2	R Core Team 2017 R: A language and environment for statistical computing. R Foundation for Statistical Computing, Vienna, Austria.	https://www.r-project.org/
R “mixOmics” package	(Le Cao et al., 2009)	http://mixomics.org/
R “random forests” package	Liaw and Wiener 2002 R news 2:18-22	https://cran.r-project.org/web/packages/randomForest/index.html

Supplemental references

Klimcakova, E., Roussel, B., Kovacova, Z., Kovacikova, M., Siklova-Vitkova, M., Combes, M., Hejnova, J., Decaunes, P., Maoret, J. J., Vedral, T., Viguerie, N., Bourlier, V., Bouloumie, A., Stich, V. and Langin, D. 2011. Macrophage gene expression is related to obesity and the metabolic syndrome in human subcutaneous fat as well as in visceral fat. Diabetologia *54***,** 876-87.

Le Cao, K. A., Gonzalez, I. and Dejean, S. 2009. IntegrOmics: an R package to unravel relationships between two omics datasets. Bioinformatics *25***,** 2855-6.

Vandesompele, J., De Preter, K., Pattyn, F., Poppe, B., Van Roy, N., De Paepe, A. and Speleman, F. 2002. Accurate normalization of real-time quantitative RT-PCR data by geometric averaging of multiple internal control genes. Genome Biol *3***,** RESEARCH0034.

Viguerie, N., Montastier, E., Maoret, J. J., Roussel, B., Combes, M., Valle, C., Villa-Vialaneix, N., Iacovoni, J. S., Martinez, J. A., Holst, C., Astrup, A., Vidal, H., Clement, K., Hager, J., Saris, W. H. and Langin, D. 2012. Determinants of human adipose tissue gene expression: impact of diet, sex, metabolic status, and cis genetic regulation. PLoS Genetics *8***,** e1002959.